Functional Identification of Nucleus Tractus Solitarius (NTS) Barosensitive Neurons: Effect of Chronic Intermittent Hypoxia (CIH)

2015

Jenya Kolpakova
University of Central Florida

FUNCTIONAL IDENTIFICATION OF NUCLEUS TRACTUS SOLITARIUS (NTS) BAROSENSITIVE NEURONS: EFFECTS OF CHRONIC INTERMITTENT HYPOXIA (CIH)

by

JENYA KOLPAKOVA
B.S. University of Central Florida, 2013

A thesis submitted in partial fulfillment of the requirements
for the degree of Master of Science
in the Burnett School of Biomedical Sciences
in the College of Medicine
at the University of Central Florida
Orlando, Florida

Fall Term
2015

Major Professor: Jack (Zixi) Cheng

ABSTRACT

Chronic Intermittent Hypoxia (CIH) is a model used to study obstructive sleep apnea (OSA). Previously, we showed that baroreflex control of heart rate (HR) (baroreflex sensitivity) is reduced in CIH rats. While afferent function and HR in response to vagal efferent stimulation are enhanced, the effect of CIH on the central components, in particular NTS, is still not completely understood. F344 rats (3-4 mo) were exposed either to CIH or room air (RA) for 35-50 days. Following CIH exposure, rats were anaesthetized with Ket/Ace. Using single-unit extracellular recording technique, we recorded NTS barosensitive neurons in response to arterial pressure (AP) changes induced by descending aorta occlusion. Our data indicated that 1) the mean arterial pressure and HR were similar in RA control and CIH groups. 2) The majority of neurons from RA and CIH NTS neurons increased firing rate, whereas other neurons decreased firing upon AP elevation. 3) In 27 RA and 31 CIH NTS neurons with increased firing rate, 15 RA and 15 CIH neurons were activated at a low ΔMAP at the early phase of AP increase (early neurons); whereas 12 RA neurons and 16 CIH neurons were activated at a late phase of AP increase (late neurons). The early neurons rapidly increased their firing during the rising phase of MAP, whereas late neurons did not increase their firing until the ΔMAP reached its peak. 4) Early neuron activity-ΔMAP relationship was further characterized by the logistic sigmoid function curve. CIH significantly increased the maximal gain of the neuron activity-ΔMAP curve and the range of the response. In addition, CIH early neurons had a significantly higher firing rate than RA early neurons, whereas CIH did not change the firing rate in late neurons. 5) For late neurons, HR reduction correlated with neuronal activity. HR reduction-neuronal activity increase curve was shifted to the right in CIH neurons, indicating that CIH decreased HR control

in response to NTS firing increase. Collectively, our data suggest that NTS barosensitive neurons have both early and late neurons, CIH selectively enhances neuron activity in response to AP changes in NTS early neurons and attenuate the baroreflex bradycardia. Along our previous work that CIH-induced the cell loss in the nucleus ambiguus (NA), we conclude that CIH attenuates the functions of NA, whereas enhances the NTS functions to compensate for the loss of function in NA.

ACKNOWLEDGEMENT

Firstly, I would like to express my sincere thanks to my thesis advisor, Dr. Zixi (Jack) Cheng. He gave me knowledge and time that enabled me to realize this project. Without his expertise and dedication it would not be possible. Dr. Cheng entrusted me with data that was a culmination of many years of his research and provided guidance to make it a reality. I am very grateful for the advice he gave me not only about my thesis, but how to be a better scientist. This knowledge that will be invaluable to me for the rest of my scientific career.

Secondly I would like to thank my committee members, Dr. Naser and Dr. Kim for assisting me with formulating my thesis project, as well as Dr. Ebert for helping me out during my Thesis Defense and making it happen. Most importantly, I would like to thank my lab members: Jin Chen and Dr. Jeff Hatcher for constant help and advice.

Last but not least I would like to thank my mother, Olga Kolpakova and my daughter Victoria Espinosa, for constant care and their belief in me. Thank you.

TABLE OF CONTENTS

LIST OF FIGURES

LIST OF TABLES

LIST OF ACRONYMS (or) ABBREVIATIONS

ADN	Aortic depressor nerve
AP	Arterial blood pressure
BPM	Beats per minute
CIH	Chronic Intermittent Hypoxia
CSP	Carotid sinus pressure
HR	Heart rate
MAP	Mean arterial blood pressure
NA	Neuronal activity
NTS	Nucleus Tractus Solitarius
PAP	Pulse arterial blood pressure
RA	Room air
SNP	Sodium nitroprusside

PART I: FUNCTIONAL IDENTIFICATION OF NUCLEUS TRACTUS SOLITARIUS (NTS) BAROSENSITIVE NEURONS

Chapter one: Introduction

The nucleus tractus solitarius (NTS) is a complex integrating center for cardiovascular regulation. Damage to the NTS effectively eliminated baroreflex control of heart rate (HR) and direct stimulation of the NTS decreased HR (Andresen and Kunze, 1994). NTS barosensitive neurons receive direct synaptic inputs from primary baroreceptor fibers that convey static and dynamic information for cardiovascular regulation (Andresen and Kunze, 1994). NTS output neurons send axons to other brainstem nuclei, such as the nucleus ambiguus and pre-sympathetic nuclei in paraventricular, caudal and rostral ventrolateral medulla, modulating the activity of these nuclei in order to control the heart rate and arterial pressure (Andresen and Kunze, 1994; Potts, 2006).

Functionally, Seagard et al. (1995) found two types of NTS neurons in mongrel dogs responding to pressure ramp increase: sudden-onset rapid-adapting neurons and slow onset non-adapting neurons. Paton et al. (2001) found the adaptive, non-adaptive neurons, and prolonged excitation NTS neurons responding to AP changes in rats. Morphologically, different types of neurons may have different structures in terms of soma size and axonal trajectory (Deuchars et al. 2000; Kawai and Senba, 1999). In addition, different NTS sensory neurons may use different neurotransmitters (Riche et al, 1990; Andresen and Kunze, 1994). The quantitative characterization of NTS barosensitive neurons indicates that NTS neurons not only encode mean arterial blood pressure (MAP), but are sensitive to the rate of AP change (Rogers et al. 1993,

1996). It was later confirmed by Zhang and Mifflin (2000) that the different rates of AP change may result in different neuronal responses in the same NTS neurons: a faster AP increase may lead to a higher response. However, the quantitative relationship of NTS barosensitive neuronal activity vs. the dynamic change of AP has not yet been well characterized.

In order to study the functional changes of different populations of barosensitive NTS neurons in disease models, it is important to define the subpopulations of NTS neurons, quantitatively characterize the NTS neuron activity (NA)-AP relationship, and examine the time-course of NTS NA upon AP changes. In this study, multiple groups of NTS neurons were identified, which responded the AP elevation differently: excitatory (majority), inhibitory or biphasic (minority). In the excitatory group, the neurons were further divided into early and late neuron subgroups according to their activation time delay. The early NA-MAP relationship, but not the late NA, was quantitatively characterized by the logistic sigmodal function. Using the time course measurement, we found that the early neurons have significantly higher firing rate in response to the late neurons. Finally, we assessed the relative contribution of early and late neurons to heart rate (HR) reduction.

Chapter two: Methodology

Animals

Fischer 344 (F344; 3–4 month) male rats were used. Procedures were approved by the University of Central Florida Animal Care and Use Committee and followed the guidelines established by the National Institutes of Health.

Surgical procedure

The procedure has been previously described in detail (Wang et al. Wang et al. 2006, 2007 and 2008; Gu et al. 2007, 2008). Briefly, rats were initially anesthetized with sodium pentobarbital (50 mg/kg i.p.). Body temperature was monitored and controlled by a rectal probe and maintained at 37 ± 1°C with a homeostatic blanket (Harvard, Holliston, MA). Supplemental doses (5 mg/kg i.v.) of sodium pentobarbital were administered (i.v) as needed to prevent eye blink and withdrawal reflexes to toe-pinch. When the animals were no longer responsive to toe-pinch, we performed the following surgical procedures. Animals were given a tracheal intubation and oxygen-enriched room air was provided through ventilation. The femoral vein was cannulated for intravenous injections of the anesthetic agent. The left common carotid artery was cannulated, and the AP was recorded and measured using a PowerLab Data Acquisition System (PowerLab/8 SP) that was connected to a pressure transducer (CB Sciences, BP100) for measurement of arterial pressure (AP). Heart rate (HR) was calculated from pulse pressure waves with the ratemeter function of LabChart 5.3 software provided with the PowerLab system. A circular arterial balloon-occluder was secured around the descending thoracic aorta which was

used to elevate AP as needed. Animals were placed in a stereotaxic instrument equipped with a head holder adapted to permit the neck to be sharply flexed. A dorsal incision was made over the neck muscles, which were retracted to expose the atlantooccipital membrane. This membrane was opened with an incision, exposing the cisterna magna and the dorsal medulla. The rostral end of the area postrema was used as a rostrocaudal reference for stereotaxic coordinates (Wang et al. 2006).

Extracellular recording of the NTS barosensitive neurons

Extracellular recording of the NTS barosensitive neurons was similar to our previous studies (Wang et al. 2006, 2007, 2008, Zhang et al, 2003, a,b). Briefly, A single-unit extracellular recording was obtained using a beveled glass micropipette (resistance 5–12 MΩ) filled with KCl (1M). With respect to calamus scriptorius, the dorsal medial NTS was located 300 μm–600 μm rostral, 300 μm–500 μm lateral, and 300 μm–500 μm ventral. The electrode was advanced using a microdrive into the dorsal medial NTS at a speed of 1–2 μm/s until single-unit activity was recorded. The spontaneous action potentials (APs) were amplified using a high impedance preamplifier (band pass 100–3,000 Hz) and fed into a window discriminator (Mentor N-750 spike analyzer), which generates a standard pulse for each spike. Potentials were visualized on an oscilloscope (model 121N; Tektronix). The pulse output of the discriminator was then fed into a rate/interval monitor (HFC) whose analog output is proportional to the number of spikes per unit time. These signals were displayed online on the computer and recorded on the data acquisition system. The sampling rate was 10,000 measurements per second (Wang et al. 2006).

Heart rate

The blood pressure catheter was connected to a blood pressure transducer (AD instruments). The transducer was positioned at the heart level. AP was measured using a PowerLab Data Acquisition System (PowerLab/8 SP) and displayed on the first channel (Fig 1A, PAP). The HR was calculated from pulse pressure in the first channel using the ratemeter function and displayed on the second channel (Fig 1A, HR). Baroreceptors were activated by the descending thoracic aortic occluder to evoke NTS barosensitive neuron response (Wang et al. 2006, 2007, 2008). Basal MAP and HR were recorded by averaging AP values and pulses for 2 min before elevation of AP. The NTS barosensitive neurons were identified by their increased activity (frequency of action potential or discharge rate) in response to transient AP elevation (24–47 mmHg) by occlusion for about 12 s. Some NTS barosensitive neurons that were inhibited by aortic occlusion were also encountered in the present study. Since our goal is mainly to study the barosensitive neurons with excitatory response to AP elevation, we did not further analyze barosensitive neurons with inhibitory or biphasic responses.

Logistic sigmoidal function curve

During aortic occlusion, mean arterial pressure (MAP), heart rate (HR) and NTS neuronal activity changes were measured. The NTS barosensitive neurons activity (NA)-ΔMAP relationship curve was fitted by logistic sigmoidal function (Kent et al. 1972). NA in response to MAP elevation was reported as the percent change relative to basal discharge using SigmaPlot 11: $Y = A/\{1 + \exp [-B(X - X_{50})]\} + Y_{min}$. where Y_{min} is the minimum value of % NTS neuronal activity relative to the basal activity, A is the range of %NTS neuronal activity (maximum -

minimum), X_{50} is the pressure at the midpoint of the range, and B is the slope coefficient. The peak slope [or Max gain ($Gain_{max}$)] was determined by: $Gain_{max} = (A)(B)/4$ and was used to evaluate the sensitivity of the NTS neural response to changes in MAP. Pressure threshold X_{th} was calculated as $X_{50} - (1.317/B)$, and pressure saturation X_{sat} was calculated as $X_{50} + (1.317/B)$, respectively. For late neurons, HR reduction-NA relationship was fitting by the logistic sigmoidal function: $Y = A/\{1 + \exp[-B (X - X_{50})]\} + Y_{max}$, where Y_{max} is the maximum reduction of the HR (bpm), A is the range of HR response (minimum - maximum), X_{50} is the % NA at the midpoint of the curve, and B is the slope coefficient. Max gain ($Gain_{max}$) = (A)(B)/4 and was used to evaluate the sensitivity of the HR reduction to NA changes. NTS NA threshold, X_{th} was calculated as $X_{50} + (1.317/B)$ and NTS NA saturation, X_{sat} was calculated as $X_{50} - (1.317/B)$, respectively.

Statistical Analysis

The average of MAP, HR, firing rate and the four parameters in the logistic function were calculated. The data are presented as mean ± SE. Comparisons between groups were made using Student's t-test or Two-way ANOVA repeated measures, Student-Newman-Keuls post hoc analysis. $P < 0.05$ was considered significant.

Chapter three: Results

Classification of NTS neurons

Data were collected from 18 animals. The baseline level mean arterial pressure (MAP) and heart rate (HR) were measured before occlusion. They were 99.6 ± 2.2 mmHg and 397.2 ± 6.4 bpm, respectively. 46 barosensitive NTS neurons were analyzed. 35 of them increased firing upon MAP increase, and were thus considered excitatory (Fig. 1A, 1B). 4 excitatory neurons were pulmonary-related barosensitive neurons. These neurons had regular basal burst activity before AP increase which was synchronized with the artificial ventilation rate (Fig. 1B). The regular basal burst activity was seen more clearly in Fig. 1B'. When we suspended ventilation for 3 s, the neuron in Fig 1B' stopped exhibiting respiratory pattern and irregular spontaneous firing appeared. After ventilation was resumed, the regular basal burst activity reappeared, which indicates the respiratory nature of the neuron. 7 other neurons decreased firing upon MAP increase and returned to basal firing rate when MAP was reduced to baseline level, and were thus described as inhibitory (Fig. 1C). The additional 4 neurons were biphasic: they decreased firing upon MAP increase, but then increased firing rate as MAP decreased to a level which was significantly higher than the basal firing rate (Fig. 1D). For some of this type of neuron, we further injected sodium nitroprusside (SNP) to decrease AP and verified that they indeed increased the firing rate concomitant with a decrease in MAP (Fig. 1E).

Excitatory neurons: ΔMAP, ΔHR and firing rate

The 35 excitatory neurons that responded with increase to AP elevation were characterized. The average MAP increase in these neurons was 37.5 ± 0.9 mmHg at a rate of 8.4 ± 0.3 mmHg/s and baroreflex bradycardia was averaged to 22.3 ± 2.6 bpm. The baroreflex sensitivity was 0.60±0.07 bpm/mmHg (ΔHR/ΔMAP). Mean baseline firing activity was 7.1 ± 0.8 spikes/s and NA had an average peak increase of 295.6 ± 35.3% relative to baseline.

Early and late activation of excitatory neurons

The majority of NTS barosensitive excitatory neurons did not increase firing rate simultaneously with MAP increase. 14 neurons increased discharge rate during the early phase of the MAP ramp increase that ranged about 3-5 s (Fig. 2A), while 21 other neurons did not significantly increase discharge rate until the MAP reached its peak plateau, which lasted for about 5-7 seconds (Fig. 2D). For the early neurons, the NA-ΔMAP relationship could be well fitted by logistic sigmodal curve ($R^2 > 0.90$) (see below). The neurons that increased firing at the later stage and could not be fitted by logistic sigmodal curve were called the late neurons. All neurons decreased firing rate during the release of the occlusion of the descending aorta. Excitatory neurons increased firing rate in response to MAP increase at different times. 5% MAP increase relative to basal pressure was defined as the reference starting time point. A 30% increase of NTS neuron firing rate relative to basal firing rate was defined as the ΔMAP-induced threshold response of NTS neuron (Wang et al. 2006). For 14 early neurons, the average ΔMAP threshold was 14.12 ± 1.65 mmHg which evoked a 30% increase of NTS neuronal firing rate relative to basal rate. For 21 late neurons, the average ΔMAP threshold was 34.07 ± 1.72 mmHg.

Early neurons were activated during MAP increase ramp and their activation delay was average within 0-2.5 s (Fig. 2B.). In contrast, the late neurons had the activation delay of 4-14 s (Fig. 2E). The distribution of peak delay from the first MAP peak to the first NA peak firing rate for the early neuron (range: -3 to 2 s) is shown in Fig. 2C, whereas the distribution of peak delay for the late neurons (range 4 to 12) is shown in Fig. 2F.

The time-course of NTS barosensitive neuronal activity

To compare the differences of NTS barosensitive neuronal activity (NA) in early and late neurons, we measured the time-course of NTS neuronal activity in response to ΔMAP. NA was calculated as the percent (%) change relative to basal discharge. ΔMAP and NA were sampled every second for up to 12 seconds during aorta occlusion-induced MAP elevation. The sec 1 and sec 2 were defined at the first data point which was <5% ΔMAP and > 5 % ΔMAP, respectively. As shown in Fig. 3A, ΔMAP was very similar in early and late neurons within 12 s. The rate of ΔMAP to the peak was also similar (early: 8.49 ± 0.6 mmHg/s, late: 8.48 ± 0.4 mmHg/s).

The basal NA of the early and late neurons was comparable (6.1 ± 1.3 vs 7.7 ± 1.1 spikes/s, $p > 0.05$). Since the rate of ΔMAP to the peak was also similar, we compared NA increase (%) and found that the early had a significantly higher increase of NA than the late neurons at 3-10 s. Noticeably, there was a trend of decline of NA within 8-12 s. The maximum NA % increases of early and late neurons were 400.2 ± 63.3% (early) and 225.8 ± 34.6% (late) ($p < 0.05$), respectively.

NTS neuronal activity (NA) – ΔMAP Relationship

To characterize the NA-ΔMAP relationship, we used the logistic sigmodal function curve. For early neurons, the NA increase-ΔMAP curve was well fitted by the logistic sigmoidal function curve (R^2= 0.90). Fig. 4A shows the original recording of an early NA in response to MAP elevation. Fig. 4A' shows a representative NA increase-ΔMAP curve of this neuron. The Table 1 included the 6 averaged parameters of the logistic function curve. Fig. 4A'' is the composite curve from the averaged parameters in Table 1 from 14 early neurons. The inset of Fig. 4A'' shows the gain distribution curve that has a $Gain_{max}$ of 29.3 %/mmHg. For the late neurons, we could not obtain NA increase-ΔMAP curve because the NA did not change until the ΔMAP reached the peak (Fig. 4B and 4B'). A 3-D plot in Fig. 4C shows the difference of the characteristic firing pattern of the two different representative early and late neurons. The early neurons increased firing to 30% at 9 mmHg of ΔMAP at 2 s, but the late neurons increased firing to 30% at 30 mmHg of ΔMAP at 4 s.

NTS neuronal activity – HR Relationship

For early neurons, the NA increase in the early phase of ΔMAP linearly correlated to the HR reduction (Fig. 5A and 5A'). Since this early neuron showed some adaption during the sustained MAP elevation (Fig. 5A), NA decreased during the late phase of ΔMAP, while the HR continued to decrease (Fig. 5A'). To show the HR reduction correlation with NA more clearly, a 3-D plot in Fig. 5B shows the HR reduction-NA relationship during a 12 s aortic occlusion from the two representative neurons shown in Fig. 4C. The early neuron correlated to the HR reduction during 12 s occlusion, whereas HR reduction did not correlate with the late NA in the

initial phase of ΔMAP, but correlated well the HR decrease in the late phase of ΔMAP (Fig. 5B). Fig. 5C was another late neuron which also shows that the HR decrease correlated with late NA. HR reduction-late NA relationship curve was well fitted using the logistic sigmoidal function. The curve of this representative late neuron is shown in Fig. 5C'. The composite curve of the 21 late neurons is shown in Fig. C'' using the averaged parameters in Table 2. The inset of Fig. 5C'' shows the Gain distribution curve with a $Gain_{max}$ of -0.23 ± 0.04. Thus, both early and late neurons contribute to HR reduction.

Chapter four: Discussion

In this study, different populations of NTS neurons were identified. The majority of the neurons increased their firing rate in response to AP elevation, whereas other neurons decreased firing rate or had biphasic responses. The heterogeneous firing patterns are consistent with other reports (Seagard et al 1995, Paton, 2001, Zhang and Mifflin, 2000). The neurons with the increased firing rate were further classified into early and late neurons according to their increase of firing rate either during the MAP elevation ramp (early) or near/after MAP reached peak (late). Using the time-course comparison, we found that the early neurons had a significantly higher firing rate than the late neurons. For the early neurons, but not for the late neurons, the NA-ΔMAP relationship curve could be fitted and characterized by six parameters of the logistic sigmodal function. Finally, the relationship of early and late neurons activity with heart rate reduction was characterized. Apparently, the early neurons contributes to HR reduction overall in the period of AP elevation (<12 s). In contrast, the late neurons activity did not contribute to the initial HR reduction but contributed to the long-lasting sustained AP elevation-induced HR

reduction after MAP reached to the plateau. It should be pointed out that the early neurons in our study showed a trend of firing adaptation to sustained AP elevation (see below discussion). But the late neurons did not show firing adaptation. The contribution of the HR reduction of the early neurons in our current study was higher than the late neurons because the early NA was higher than the late NA during the entire 12 s of occlusion (Figs. 3 and 5B). If early NA further adapts to a larger, prolonged MAP elevation, the late neurons might contribute more the baroreflex bradycardia. This assumption should be tested in the future.

Classification of NTS barosensitive neurons

Majority of neurons (35 out of out of 46, including 4 pulmonary-related neurons) increased firing upon AP elevation. In contrast, 7 neurons decreased firing. Additionally, 4 neurons appeared to have a bi-phasic response: decreased firing rate upon AP elevation but increased firing rate following AP decrease. We also found some neurons increased firing rate during SNP-induced decrease of MAP (Fig. 1F). Similar types of NTS barosensitive neurons were reported by Zhang and Mifflin (2000), who also found that the NTS neurons increase discharge rate, decreased discharge rate or are bi-phasic in response to MAP elevation, as well as other neurons which increased or decreased firing rate in response to a SNP-induced MAP depression. Seagard et al. (2001) also reported some neurons with decrease in firing rate in response to carotid MAP elevation.

In our study, after the MAP reached the threshold, the excitatory neurons had a sudden-onset activity which reached the peak within 3-5 sec. This rapid increase of firing is similar to the sudden-onset neurons as reported by Seagard et al (1995, 2001). But our neurons only show

small adaptation as shown in Fig. 1A. In contrast, Seagard's sudden-onset neurons showed much more significant adaptation to a large pressor ramp increase. This difference could be due to the difference in methodology: our MAP was first increased by 30-50 mmHg from the baseline MAP and then held relatively constant at 130-150 mmHg. In contrast, Seagard et al (1995) had a ramp carotid sinus pressure (CSP) increase from 0 to 250 mmHg and the neurons were silent up to a given CSP (67.8-98.1 mmHg) in dogs, and then responded with burst of activity which immediately decreased as the ramp continued. Therefore, our NTS neurons only showed the trend but did not show as much as adaptation possibly due to our relatively small increase of MAP compared to the large increase CSP in Seagard et al (1995, 2001). Interestingly, some excitatory neurons displayed evoked hyperpolarization after MAP return to its baseline as reported by Paton et al. (2001) (Fig. 1A, and Fig. 4A).

Early and late NTS neurons

We observed that 14 neurons (out of 35) increased firing rate during the early phase of AP increase (early neurons; Fig. 2A and Fig. 4A), whereas the remaining 21neurons increased firing rate only later near/after AP elevation reached its peak (late neurons; Fig. 2D and Fig 4B). The early and late neurons had similar basal firing rate, ΔMAP and rate of MAP increase (Fig. 3A). Interestingly, the early neurons had higher firing rate increase in response to the MAP elevation compared to the late neurons during the period of AP elevation (<12 s) before the occlusion was released. Our early and late activation NTS neurons are consistent with Zhang and Mifflin (2000) who reported that in response to MAP increase, the peak discharge of NTS barosensitive neurons occurred either near/ after MAP reached the peak in both monosynaptic

(before/during 5 vs. after 19 neurons) and polysynaptic neurons (near 5 vs. after 14 neurons). For the late NTS neurons, the delay from the point where the MAP reached the maximum to the peak of discharge was 4-12 seconds, which was similar to the reported delay in Zhang and Mifflin (2000). The differences in activation could not simply be due to monosynaptic vs polysynaptic inputs to NTS neurons, since Zhang and Mifflin (2000) found that NTS neurons with both monosynaptic vs. polysynaptic inputs had similar early and delayed firing patterns to the early and late neurons in our study. Additionally, it is not likely that the conduction velocity difference between myelinated and non-myelinated baroreceptor primary fibers could determine the early and delayed response time, as the time from the activation of the baroreceptor depressor A- or C-nerve fiber terminals in the aortic arch and carotid body to the NTS would be less than a second. Previously, we labeled aortic depressor nerve innervation of the aortic arch and observed that there are much less large aortic depressor nerve fibers than small ones (Cheng et al. 1997; Li et al. 2010). This observation is consistent with Brown (1980), who reported that there are less A-fibers than C-fibers in the depressor nerve. In our study, we had less early neurons than late neurons. Since C-type axons have much higher threshold than A-fibers (Brown, 1980), we suggest that the early neurons may receive A-fiber inputs and late neurons may receive C-fiber inputs. However, this hypothesis should be tested in a future experiment.

The early neurons may have low threshold neurons in the sense that they can be rapidly activated by a small increase of MAP. In contrast, the latest neurons did not even start to increase their firing rate from the baseline until the MAP increases reached its' plateaus. We postulated that these late neurons may have had a high threshold because they could not be activated until they were stimulated by a large MAP increase for a certain amount of time. For example, some

late neurons started to increase discharge rate only after the MAP reached the plateaus for several seconds. Therefore, late neurons might have used temporal summation of the sustained MAP elevation.

Previously, Seagard et al., (1990) reported that there are two types of baroreceptors, which have either a sigmoidal or a hyperbolic relationship with increases in carotid sinus pressure and have different activation thresholds. Later, two types of NTS barosensitive neurons were identified (Seagard et al., 2001): rapidly adapting neurons which have a sudden onset firing after the pressure reaches the threshold and begin to adapt in firing as the pressure continues to increase up to 250 mmHg, whereas the slow-onset non-adapting neurons have a higher threshold than the other type and continuously and slowly increase their firing rate as the pressure increases to 250 mmHg. Again, Seagard et al., (1990) used a continuous ramp pressure increase as the stimulus, whereas we used a transient increase of MAP changes with a much lower range, therefore, adaptation of NTS neurons in our study might not be as obvious as the one shown in Seagard et al., (1990) study.

Andresen and Peters (2008) found that NTS neurons have single distinct threshold intensities, responses which are activated by a single-afferent axon, and no additional contacts were recruited by stimulus intensity increases. Recently, Chen et al., (2014) reported that there was actually a continuum of activation thresholds of aortic baroreceptors. In our study, we found that there is a continuous activation delay for early and late neurons (Fig. 2A). Therefore, our report of NTS neurons which increase firing at different pressure thresholds may echo the

distribution of activation thresholds of primary baroreceptor depressor nerves (Chen et al., (2014).

Time-course of NTS barosensitive neuronal activity (NA)-ΔMAP increase

To further characterize the functional NTS NA, we examined the time-course of NA-ΔMAP increase. Time-course depicts the relationship between NTS neuronal activity and MAP increase even after the MAP reaches the plateau and neurons continue to increase discharge frequency. In contrast to the sigmoidal logistic function which only applied to the early neurons, time-course measurement was applied to both early and late neurons. As shown in Fig. 3B, the time-course can be used to compare NTS neurons activity between two types of neurons. Early neurons did not only have a rapid activation, but also showed a significantly higher firing rate in response to MAP increase.

NTS neuronal activity and heart rate reduction

Whether and how the firing of early and late neurons may contribute to the decreased heart rate is an issue. Apparently, rapid firing of early neurons during MAP increase correlates nicely with the initial drop of the heart rate. As shown in the time-course measurement, MAP reached the plateau at about 5 s (Fig. 3A), but the firing of the early neurons reached the peak at 5-6 s, and began to adapt at 8-12 s (Fig. 3B), whereas the heart rate continued to drop till 12 s when the occluder was released and AP started to drop (Fig. 5A). Therefore, in the initial stage of MAP elevation, the firing rate of the early neurons increased in correlation with HR reduction linearly (Fig. 5A'). But at the later stage of MAP elevation, the firing rate of early neuron went

down in general whereas HR still decreased as shown in Fig. 5A' with arrows. In contrast, in the initial stage of MAP elevation, the late neurons did not increase their firing significantly, but they increased firing, as shown with arrows in Fig. 5B. To further expose the relationship of the firing of late neurons with the heart rate reduction, we used the sigmodal logistic function to fit the data. In contrast to the early neurons, the late neurons were not related to the initial heart rate drop, but strongly correlated with the later heart rate reduction of the fitting curve (Fig. 5C'). We suggest that the early neurons contribute to both the initial and late stages of HR reduction, whereas the late neurons contributed mainly to the late stages of HR drop. Compared to the firing rate as shown in Fig. 3, it appears that the early neurons may contribute to heart rate reduction more than the late neurons. However, it should be pointed out that if the MAP elevation had lasted even longer, then the adaptation of early neurons could have become more significant and the firing rate of the early neurons would be less than the late neurons, which may not adapt. In our study, we found more late neurons than early neurons, which was consistent with the finding by Zhang and Mifflin (2000). If the NTS uses population coding to regulate the HR, then we would speculate that the early neurons play the major role in the initial control of the heart rate and may reduce their contribution to long-lasting sustained high arterial pressure elevation. In contrast, the late neurons may not be activated to contribute to the initial control of the heart rate, but are likely to be more responsive to long-lasting sustained high arterial pressure elevation.

Chapter five: Conclusion

In Part I, we have identified serval types of neurons that have different properties in firing patterns in response to arterial pressure changes. The majority of these neurons are early and late neurons which increase the fringe rate in response to arterial pressure elevation. Using the activation and peak delay, logistic sigmodal function and time-course, we have differentiated, characterized and compared the early and late neurons. The correlation of the early and late neurons activity with the heart rate reduction suggest that these neurons may contribute to HR reduction differently. Our data will provide a further understanding of NTS barosensitive neuron function. Previously, we used the sigmoidal logistic curve to characterize and compare aortic baroreceptor depressor nerve function and renal sympathetic nerve function in normal and chronic intermittent hypoxia and diabetic animals (Gu et al., 2007, 2008, 2009). However, the functional changes in the NTS barosensitive neurons have not yet been fully characterized. Therefore, we have applied these methods to elucidate the functional difference of the NTS barosensitive neurons in disease models, such as Chronic Intermittent Hypoxia (CIH; Kolpakova et al., 2015) as shown in Part II.

PART II: EFFECTS OF CHRONIC INTERMITTENT HYPOXIA (CIH) ON NTS BAROSENTIVE NERUONS

Chapter six: Introduction

Obstructive sleep apnea (OSA) affects up to 24% of males and 9% of females (Bradley and Floras, 2009) and is associated with substantial morbidity in the central nervous system and cardiovascular systems (Young et al., 1997; Roux et al., 2000). Baroreflex control of heart rate is significantly impaired in OSA patients and can lead to heart failures and hypertension (Parati et al., 1997; Bonsignore et al., 2006; Monahan et al., 2006). Chronic intermittent hypoxia (CIH) has been used as a common animal model for sleep apneas because of the recurring hypoxic episodes associated with OSA (Gozal et al., 2001). Similarly to OSA, CIH-treated animals have reduced baroreflex sensitivity (Lai et al., 2006). Therefore, a thorough understanding is required for improvement and treatment strategies of OSA and its associated symptoms.

Previously, we have demonstrated that following CIH exposure of Fischer 344 (F344) young adult rats, the baroreflex control of heart rate (HR) was significantly attenuated (Gu et al., 2007; Lin et al., 2007; Yan et al., 2008; Yan et al., 2009). The impairment of baroreflex response is not due to the deficit of aortic depressor nerve function, which was actually found to be augmented in rats and mice (Gu et al., 2007). Neither was CIH-attenuated baroreflex response due to vagal efferent cardiac nerve degeneration in the heart because direct vagal efferent stimulation actually resulted in an enhanced heart rate response (Lin et al., 2007). The evidence that a decrease in bradycardic response to ADN stimulation implies that the central component is responsible for CIH-induced impairment of baroreflex control of heart rate (Gu et al., 2007).

Baroreceptive afferent fibers make their first synapses onto Nucleus tractus solitarius (NTS) neurons. Therefore NTS is the utmost important integrating site of baroreceptive stimuli (Andresen and Kunze, 1994). Nucleus ambiguus (NA) have been largely characterized in terms of its contribution to CIH-induced impairments (Lin et al., 2008; Yan et al., 2008; Yan et al., 2009), however, NTS role has not been well established. Several studies point to an altered function of NTS neurons (Reeves et al., 2006b; de Paula et al., 2007b; Kline et al., 2007; Zhang et al., 2008; Almado et al., 2012). However, whether CIH alter NTS activity in response to arterial pressure changes have not yet been examined. Here, we report that CIH increases barosensitive NTS neurons' activity in response to arterial pressure changes in anesthetized rats.

Chapter seven: Methodology

Animals

Fischer 344 (F344; 3–4 month) male rats were used. Procedures were approved by the University of Central Florida Animal Care and Use Committee and followed the guidelines established by the National Institutes of Health.

Intermittent Hypoxia exposure

F344 rats were exposed to room air or intermittent hypoxia for 35-50 days. The intermittent hypoxia (IH) profile consisted of alternating 21% (90s) and 10% oxygen (90s) every 6 min for the duration of the light cycle and maintained at 21% oxygen for the night period

(12h:12h). The room air (RA) control animals were housed in room air under the same conditions as CIH-exposed animals, except the concentration of oxygen was maintained throughout the duration of exposure.

Surgical procedure

The procedure has been previously described in detail (Wang et al, 2006, 2007 and 2008; Gu et al. 2007, 2008). Briefly, rats were initially anesthetized with Ketamine/Acepromazine (50 mg/kg i.p.). Body temperature was monitored and controlled by a rectal probe and maintained at 37 ± 1°C with a homeostatic blanket (Harvard, Holliston, MA). Supplemental doses (5 mg/kg i.v.) of sodium pentobarbital were administered (i.v) as needed to prevent eye blink and withdrawal reflexes to toe-pinch. When the animals were no longer responsive to toe-pinch, we performed the following surgical procedures. Animals were given a tracheal intubation and oxygen-enriched room air was provided through ventilation. The femoral vein was cannulated for intravenous injections of the anesthetic agent. The left common carotid artery was cannulated, and the AP was recorded and measured using a PowerLab Data Acquisition System (PowerLab/8 SP) that was connected to a pressure transducer (CB Sciences, BP100) for measurement of arterial pressure (AP). Heart rate (HR) was calculated from pulse pressure waves with the ratemeter function of LabChart 5.3 software provided with the PowerLab system. A circular arterial balloon-occluder was secured around the descending thoracic aorta which was used to elevate AP as needed. Animals were placed in a stereotaxic instrument equipped with a head holder adapted to permit the neck to be sharply flexed. A dorsal incision was made over the neck muscles, which were retracted to expose the atlantooccipital membrane. This membrane

was opened with an incision, exposing the cisterna magna and the dorsal medulla. The rostral end of the area postrema was used as a rostrocaudal reference for stereotaxic coordinates (Wang et al. 2006).

Extracellular recording of the NTS barosensitive neurons

Extracellular recording of the NTS barosensitive neurons was similar to our previous studies (Wang et al. 2006, 2007, 2008, Zhang et al, 2003, a,b). Briefly, A single-unit extracellular recording was obtained using a beveled glass micropipette (resistance 5–12 MΩ) filled with KCl (1M). With respect to calamus scriptorius, the dorsal medial NTS was located 300 μm–600 μm rostral, 300 μm–500 μm lateral, and 300 μm–500 μm ventral. The electrode was advanced using a microdrive into the dorsal medial NTS at a speed of 1–2 μm/s until single-unit activity was recorded. The spontaneous action potentials (APs) were amplified using a high impedance preamplifier (band pass 100–3,000 Hz) and fed into a window discriminator (Mentor N-750 spike analyzer), which generates a standard pulse for each spike. Potentials were visualized on an oscilloscope (model 121N; Tektronix). The pulse output of the discriminator was then fed into a rate/interval monitor (HFC) whose analog output is proportional to the number of spikes per unit time. These signals were displayed online on the computer and recorded on the data acquisition system. The sampling rate was 10,000 measurements per second (Wang et al. 2006).

Heart Rate

The blood pressure catheter was connected to a blood pressure transducer (AD instruments). The transducer was positioned at the heart level. AP was measured using a PowerLab Data Acquisition System (PowerLab/8 SP) and displayed on the first channel (Fig 1A, PAP). The HR was calculated from pulse pressure in the first channel using the ratemeter function and displayed on the second channel (Fig 1A, HR). Baroreceptors were activated by the descending thoracic aortic occluder to evoke NTS barosensitive neuron response (Wang et al. 2006, 2007, 2008). Basal MAP and HR were recorded by averaging AP values and pulses for 2 min before elevation of AP. The NTS barosensitive neurons were identified by their increased activity (frequency of action potential or discharge rate) in response to transient AP elevation (24–47 mmHg) by occlusion for about 12 s. Some NTS barosensitive neurons that were inhibited by aortic occlusion were also encountered in the present study. Since our goal is mainly to study the barosensitive neurons with excitatory response to AP elevation, we did not further analyze barosensitive neurons with inhibitory or biphasic responses.

Logistic sigmoidal function curve

During aortic occlusion, mean arterial pressure (MAP), heart rate (HR) and NTS neuronal activity changes were measured. The NTS barosensitive neurons activity (NA)-ΔMAP relationship curve was fitted by logistic sigmoidal function (Kent et al. 1972). NA in response to MAP elevation was reported as the percent change relative to basal discharge using SigmaPlot 11: $Y = A/\{1 + \exp [-B(X - X_{50})]\} + Y_{min}$. where Y_{min} is the minimum value of % NTS neuronal activity relative to the basal activity, A is the range of %NTS neuronal activity (maximum -

minimum), X_{50} is the pressure at the midpoint of the range, and B is the slope coefficient. The peak slope [or Max gain ($Gain_{max}$)] was determined by: $Gain_{max} = (A)(B)/4$ and was used to evaluate the sensitivity of the NTS neural response to changes in MAP. Pressure threshold X_{th} was calculated as X_{50} - (1.317/B), and pressure saturation X_{sat} was calculated as X_{50} + (1.317/B), respectively. For late neurons, HR reduction-NA relationship was fitting by the logistic sigmoidal function: $Y = A/\{1 + \exp[-B (X - X_{50})]\} + Y_{max}$, where Y_{max} is the maximum reduction of the HR (bpm), A is the range of HR response (minimum - maximum), X_{50} is the % NA at the midpoint of the curve, and B is the slope coefficient. Max gain ($Gain_{max}$) = (A)(B)/4 and was used to evaluate the sensitivity of the HR reduction to NA changes. NTS NA threshold, X_{th} was calculated as X_{50} + (1.317/B) and NTS NA saturation, X_{sat} was calculated as X_{50} - (1.317/B), respectively.

Statistical Analysis

The average of MAP, HR, firing rate and the four parameters in the logistic function were calculated. The data are presented as mean ± SE. Comparisons between RA and CIH groups were made using Student's t-test or Two-way ANOVA repeated measures, Student-Newman-Keuls post hoc analysis. $P < 0.05$ was considered significant.

Chapter eight: Results

Classification of NTS neurons

Data were collected from 10 RA and 11 CIH animals. The baseline level mean arterial pressure (MAP) and heart rate (HR) were measured for RA and CIH animals before occlusion. The baseline MAP for RA and CIH animals were not significantly different: 99.5±2.9 vs 104.3±2.4 vs mmHg. Baseline HR for RA and CIH animals were 324.27±4.5 and 334.71±6.0 bpm, respectively. 34 RA and 39 CIH neurons were analyzed. 27 of RA neurons and 31 CIH neurons increased firing upon MAP increase, and were thus considered excitatory (Fig. 6A). 4 RA and 5 CIH excitatory neurons were pulmonary-related barosensitive neurons. These neurons had regular basal burst activity before AP increase which was synchronized with the artificial ventilation rate (Fig. 6B). Other neurons decreased firing rate upon MAP increased and returned to the basal firing rate when MAP went back to baseline level and were thus described as inhibitory: 3 RA and 6 CIH inhibitory neurons (Fig. 6C) were found. Still other neurons increased firing upon MAP decrease, and we found 4 RA and 2 CIH neurons of this type (Fig. 6D). For some of this type of neurons, we further injected sodium nitroprusside (SNP) to decrease AP and verified that they indeed increase the firing rate with the decrease in MAP (Fig. 6E).

The time-course of NTS excitatory RA and CIH neuronal activity (NA).

To compare the differences in NTS barosensitive neuronal activity (NA) between RA and CIH neurons, we determined not only whether maximum NTS response was affected by CIH,

but how the NTS neuronal response differed every second during MAP elevation. Thus we constructed a time-course of only early NTS neuronal activity % increase relative to baseline in response to MAP elevation measured and averaged at 1 s interval. We measured the time-course of NTS neuronal activity in response to ΔMAP (Fig. 7). NA was calculated as the percent (%) change relative to basal discharge. ΔMAP and NA were sampled every second for up to 12 seconds during aorta occlusion-induced MAP elevation. The sec 1 and sec 2 were defined at the first data point which was between <5% ΔMAP and >5 % ΔMAP, respectively. As shown in Fig. 7A, ΔMAP was very similar in RA and CIH neurons within 12 s. The average MAP increased in RA neurons was 27.5±1.4 mmHg and 27.7±1.1 mmHg for CIH neurons. The rate of ΔMAP to the peak was also similar (RA: 6.94±0.82 mmHg/s, CIH: 6.73±0.80 mmHg/s).

The basal NA of the early and late neurons was comparable (7.23±1.30 spikes/s for RA and 6.67±1.13 spikes/s for CIH neurons, $P > 0.05$). Since the rate of ΔMAP to the peak was also similar, we compared NA increase (%) and found that the CIH neurons had a significantly higher increase of NA than the RA neurons at 7-12 s. The maximum NA % increases was significantly higher for CIH neurons than for RA: 189.4± 24.8 % for CIH vs 131.8 ± 11.2% for RA ($P < 0.05$).

Early and late activation of excitatory neurons

The NTS barosensitive excitatory neurons did not increase firing rate simultaneously with MAP increase. 15 RA and 15 CIH neurons increased discharge rate (30% relative to baseline; Wang et al. 2006) during the early phase of the MAP ramp increase that ranged about 3-5 s (Fig. 8A, B), while the remaining 12 RA and 16 CIH excitatory neurons did not

significantly increase discharge rate until the MAP reached its peak plateau, which lasted for about 5-7 seconds (Fig. 8C, D). For the early neurons, the NA-ΔMAP relationship could be well fitted by logistic sigmodal curve (R^2>0.88) (see below). The neurons that increased firing at the later stage and could not be fitted by logistic sigmodal curve were thus called the late neurons. All neurons decreased firing rate during the release of the occlusion of the descending aorta.

CIH increased *early* neurons' response to arterial blood pressure elevation

To characterize the NA increase-ΔMAP relationship of early RA and CIH neurons, we used the time-course and logistic sigmodal function curve. Fig. 9A shows the original recordings of early NA in response to MAP elevation in RA and CIH neurons. As described above, for the time-course of NTS neuronal activity, NA was calculated as the percent (%) change relative to basal discharge. ΔMAP and NA were sampled every second for up to 12 seconds during aorta occlusion-induced MAP elevation. As shown in Fig. 9B, ΔMAP was very similar in RA and CIH neurons within 12 s. The average MAP increased in RA neurons was 26.6± 1.4 mmHg at a rate of 5.6± 0.6 mmHg/s and for CIH neurons was 26.8±1.4 mmHg at a rate of 6.3± 1.1 mmHg/s. Since the basal NA of the early was also comparable (7.2± 1.9 spikes/s for RA and 6.7± 1.8 spikes/s for CIH neurons, $P > 0.05$), we compared NA increase (%) and found that the CIH neurons had a significantly higher increase of NA than the RA neurons at 5-12 s, 2 seconds faster than when early and late neurons were combined (Fig. 7B). The maximum NA % increases was also significantly higher for CIH neurons than for RA: 203.3± 34.8% for CIH vs 122.5± 16.4% for RA ($P < 0.05$).

Fig. 9D shows a representative NA increase-ΔMAP curve and the six averaged parameters of the logistic function curves for 15 RA and 15 CIH neurons are summarized Table 3. Fig. 9E is the composite curve from the averaged parameters in Table 3 from 15 early RA and CIH neurons. As can be seen from the composite curves in Fig. 9E and exemplified in single neurons curve in Fig. 9D, CIH neurons had significantly higher NA increase (% relative to baseline; range) and $Gain_{max}$. The inset of Fig. 9E shows the gain distribution curve that has a $Gain_{max}$ of 19.1±4.2 %/mmHg for RA and 47.7±12.6 %/mmHg for CIH.

CIH did not alter the response of late barosensitive neurons to MAP increase, but induced changes in NTS neuronal activity – HR relationship

Similarly to the data above, we characterized the NA increase-ΔMAP relationship of 12 RA and 16 CIH late neurons. Fig. 10A shows the original recordings of NA in response to MAP elevation in RA and CIH late neurons. The basal NA of the early was comparable (7.0± 1.6 spikes/s for RA and 6.6± 1.4 spikes/s for CIH neurons, $P > 0.05$). Maximum ΔMAP increase and rate was comparable between the two groups: 26.0±2.3 mmHg increase at a rate of 8.6±1.5 mmHg/s for RA neurons and 26.9± 1.3 mmHg increase at a rate of 7.1±1.2 mmHg/s for CIH neurons. In contrast to early neurons, the maximum NA% increase was not significantly different between two groups (170.2±37.2% increase for CIH compared to 151.7±18.2 % increase in RA neurons). Moreover, time-course of NTS NA over 12 s of MAP increase (Fig. 10B) revealed no significant difference at any time-point of NA response (Fig. 10C). Therefore, the significant increase that was seen in all neurons (early and late; Fig. 7B), was mostly due to early neurons' increase in firing rate.

For the late neurons, we could not obtain NA increase-ΔMAP curve because the NA did not increase until the ΔMAP reached the peak. Interestingly, although the ΔMAP reached the peak, heart rate (HR) continued to decrease for several seconds longer. Consequently, the late neurons showed correlation with baroreflex bradycardia in the late phase of ΔMAP. To examine HR-NA relationship, we construction HR reduction-NA increase curve was well fitted using the logistic sigmoidal function for RA and CIH neurons. The curves of these representative late neurons are shown in Fig. 10D. The composite curves of 12 RA and 16 CIH late neurons are shown in Fig. 5E using the averaged parameters in Table 2. Interestingly, we found that X_{50}, mid-point NTS neuronal activity value of the curve, was significantly shifted to the right: 64.9±11.9% for CIH neurons compared to 35.1±6.2% for RA neurons (Fig. 10E & Fig. 10E inset). Additionally, NTS NA saturation value (X_{sat}) was significantly higher for CIH neurons.

Chapter nine: Discussion

Previously, our work implied that the central components of the baroreflex loop is impaired in CIH rats (Gu et al., 2007, Yan et al. 2008, 2009). However, the effect of CIH on NTS which is the first integration center and directly receives baroreceptor input has not yet been well elucidated. Here, we examined the effect of CIH on firing rate of barosensitive NTS neurons. The majority of neurons recorded were excitatory for CIH and RA groups, which responded to MAP elevation with an increase in firing rate. These excitatory neurons can be further classified into early and late neurons according to whether the increased the firing rate during the MAP elevation ramp (early neurons) or near/after MAP reached peak (late neurons). Using the maximum response and time-course comparison, we found that early CIH neurons had

a significantly higher firing rate than early RA neurons, whereas late CIH neurons showed no significant difference in firing rate compared to late RA control. For early neurons, the neuronal activity (NA)-ΔMAP relationship curve was well fitted and characterized using the six parameters of the logistic sigmodal function curve. In CIH, neuronal response range (% baseline) and a maximum slope of the curve (Gainmax) were significantly enhanced. Finally, the relationship of late neuronal activity-HR reduction was characterized using logistic function curve. CIH right-shifted HR reduction-NTS neuronal activity increase curve, suggesting that CIH decreases NTS control over the heart rate.

CIH did not alter baseline activity and the activation time of the NTS early and late neurons in response to MAP elevation

In this study, we found that the majority of neurons in RA (27 out of 34) and CIH (31 out of 39) groups, including a few pulmonary-related neurons, increased firing upon MAP elevation. In contrast, 3 RA and 6 CIH neurons decreased firing rate during MAP elevation. Additionally, 4 RA and 2 CIH neuron increased firing rate following MAP decrease. We also found some neurons increased discharge rate during SNP-induced decrease of MAP (Fig. 5E). Similar types of NTS barosensitive neurons were previously reported by Zhang and Mifflin (Zhang and Mifflin, 2000).

We also observed that 15 RA neurons (out of 27) and 15 CIH neurons (out of 31) increased firing rate during the early phase of MAP increase (early neurons), whereas the remaining 12 RA and 16 CIH neurons increased firing rate only later near/after MAP elevation reached its peak (late neurons). The early and late neurons had similar basal firing rate, ΔMAP

and MAP increase rate in RA and CIH groups. Our finding of early and late NTS neurons are consistent with Zhang and Mifflin (Zhang and Mifflin, 2000), who reported that in response to MAP increase, the peak discharge of NTS barosensitive neurons occurred either before/during, or after MAP reached its peak in both monosynaptic (5 'before/during' vs. 19 'after' neurons) and polysynaptic neurons (5 'before/during' vs. 14 'after' neurons; (Zhang and Mifflin, 2000). It is not likely that the conduction velocity difference between myelinated and non-myelinated baroreceptor primary fibers could completely determine the early and delayed response time, as the time from the activation of the baroreceptor depressor A- or C-nerve fiber terminals in the aortic arch and carotid artery to the NTS would be less than a second (Brown, 1980; Paton, 1998; Striedter, 2014). Our data indicated CIH did not affect the baseline activity of barosensitive NTS early and late neurons, and the activation time of the NTS response to MAP elevation for early and late neurons were also similar.

CIH significantly increased NTS Barosensitive Early Neuron Function

To characterize NTS neuronal activity, we examined the time-course of neuronal activity-ΔMAP relationship. The time-course depicts the relationship between NTS neuronal activity and MAP elevation from the time when neuron activity increased 30% above the basal activity till 12 seconds when MAP started to decline due to the release pressure of descending aorta occlutor. First, we measured the time-course response of all excitatory neurons (both early and late neurons), and found that CIH induced significant increase firing rate during 12 sec aortic occlusion. Next, we examined the effect of CIH in early and late neurons separately. Interestingly, only the early CIH neurons showed a significantly higher increase in firing

compared to RA, whereas late CIH neuron response was similar to RA control. To further understand CIH-induced increase in early neurons discharge rate, we used the sigmoidal logistic function to construct the early NA-ΔMAP curves for CIH and RA NTS early neurons. For late neurons, however, we could not construct a NTS NA-ΔMAP relationship curve because the MAP had almost or already reached the plateau before NTS neurons started to increase firing. Consistent with time-course measurements, we found that CIH significantly increased the range of the neuronal activity and maximum gain ($Gain_{max}$) compared to RA control. Thus, CIH significantly increased NTS early neuron baroreceptive function.

For the late neurons, they could not be activated until they were stimulated by a large MAP increase for a certain amount of time (up to 5 s). Therefore, they might be neurons with a higher threshold activation (Andresen and Peters, 2008), or they might receive the input from high threshold baroreceptor afferent (Chen et al., 2014). Since depressor A-fibers have low activation threshold and C-fibers have a much higher activation threshold than A-fibers (Brown, 1980), it is likely that A-fibers and C-fibers may contribute to NTS early and late neruons, respectively. Further experiments are needed to identify the differential pathways from baroreceptor afferent nerves to early and late neurons in NTS as well as their roles in controlling the heart. In our study, CIH appears to affect the two pathways differently.

It is difficult to offer the exact cause for the difference in CIH effect on early vs. late neurons at this moment. Further study is needed to elucidate the cause. However, NTS are composed of many different neuron, neurotransmitter and receptor types (Andresen and Kunze, 1994; Kline, 2008), and it is likely that CIH may affect NTS subpopulations differently.

Previously, it has been demonstrated that CIH enhances response to AMPA receptor activation, whereas decreased the response of NMDA receptors in the same NTS chemosensitive neurons (de Paula et al., 2007a). Chemoreceptor afferent from carotid body projects to commissural nuclei of NTS and baroreceptor afferent from carotid sinus and aortic arch projects to dorsal medial nuclei of NTS. CIH clearly increased chemoreceptor afferent activity inputs to NTS chemosenstive neurons (Kline 2010). Within NTS, there are different populations of neurons: chemosenstive and barosensitive among many other senses. In addition, one NTS neuron may employ multiple receptors for different neurotransmitters. Currently, the issue of whether CIH increases or decrease NTS neuron response to electrical and chemical stimulation is controversial, depending upon different receptors and population of neurons. De Paula et al (2007) reported that CIH increased AMPA-evoked current but decreased NMDA-evoked currents of the same NTS neurons which directly receive carotid body chemoreceptor inputs in in vitro brain slice. Kline et al. (2007) found that CIH induces an increase in NTS postsynaptic cell activity initiated by spontaneous presynaptic transmitter release that is accompanied by an increase in firing rate of secondary NTS neurons in response to electrical stimulation of the solitary tract in brain slices (see Kline 2010 for a review). In contrast, Almado et al. (2012) reported that CIH depresses afferent neurotransmission in NTS neurons by a reduction in the number of active synapses. While the differences of different studies are not easy to interpret, it appears that Kline et al. (2007) and Almado et al. (2012) recorded different publications of neurons in the NTS and CIH has different effects on different NTS neurons.

Thus far, the effect of CIH-induced changes of chemoreceptor afferent and NTS chemosensitive neurons have been examined in numerous studies, whereas the studies aimed at

CIH-induced changes of baroreceptor afferent and NTS barosensitive neurons were much less studied (see Kline et al 2010; 2014 review). Previously, we have studied CIH-induced changes of multiple neuronal components in the baroreflex arc in a series of studies (Gu et al. 2007, Lin et al 2007, 2008, Ai et al. 2008, 2009, Yan et al. 2008, 2009, see Kline et al 2010; 2014 review of our work). Along this line of study, our current data suggest that CIH has differential effects on different population of NTS neurons: CIH increases early barosensitive neurons activity in response to AP elevation, whereas does not change late barosensitive neurons activity.

Late NTS neurons activity and heart rate reduction

To illustrate the relationship of the late neuron activity with HR reduction, we used the sigmoidal logistic function curve to fit the HR reduction-late neuron activity relationship. The discharge rate of the late neurons correlated well with HR decrease in both RA and CIH groups. Interestingly, CIH significantly increases X50, indicating that CIH shifted the relationship curve rightward. These findings suggest that NTS late neurons activity may significantly contribute to the heart rate reduction in addition to the early neurons. Very importantly, CIH significantly reduced the NTS regulation of baroreflex bradycardia. Since CIH enhanced NTS early neurons and did not change late neuron function, this data suggests that the later neural components in the baroreflex loop after NTS (such as the nucleus ambiggus) may be responsible for the baroreflex impairment.

Chapter ten: Conclusion

Previously, we have established that CIH impairs baroreflex control of the heart rate (HR). In baroreflex arc, there are multiple neural components, including baroreceptor afferent neurons, NTS barosensitive neurons, vagal motor neurons from nucleus ambiguus, and cardiac ganglia. To test which components were altered by CIH, we have systematically examined aortic depressor afferent nerve, vagal efferent nerve and central components. Our previous data indicate that CIH impairs the central components (possibly NTS and/or nucleus ambiguus), whereas the peripheral components are enhanced, i.e., aortic depressor afferent nerve function and HR responses to vagal efferent nerve stimulation are increased (Gu et al., 2007, Lin et al., 2007). Associated with the functional enhancement of the peripheral components, CIH increases baroreceptor afferent nerve innervation of the aortic arch and vagal efferent projection to cardiac ganglia (Lin et al. 2008, Ai et al. 2009). Along with the functional impairment of the central components, CIH decreases the HR responses to the excitatory neurotransmitter L-glutamate microinjection into the nucleus of ambiguus to activate cardiac motor neurons to control the heart which is associated with the cell loss of glutamatergic receptors (AMPA and NMDA) – immunoreactive and Nissl-Stained vagal cardiac motor neurons in the nucleus of ambiguus (Yan et al., 2008, 2009). However, the functional changes of NTS barosensitive neurons had never been tested in our previous studies.

In this study, we examined the effect of CIH on the firing rate of barosensitive NTS early and late neurons. CIH significantly increased barosensitive NTS early neuron function but did not change barosensitive NTS late neuron function. It appeared that the early neuron activity contributes to the initial phase of HR reduction (before the MAP elevation reaches plateau) as

well as a later phase of the HR reduction (after the MAP elevation reaches plateau) (see Project I). For late neurons, the activity of the late neurons and HR reduction relationship can be well correlated and fitted using the logistic function curve. CIH significantly shifted the relationship curve rightward and hence decreased the NTS control over the HR. Since CIH increases NTS early neuron function and does not change NTS late neuron function as shown in this study, and since CIH increases the vagal efferent nerve control over HR but decreases the control of vagal cardiac motor neurons in the nucleus ambiguus over the HR (Gu et al. 2008; Lin et al. 2007, Yan et al. 2008, 2009), we now can draw a clear conclusion: CIH impairs baroreflex control of HR mainly due to the degeneration of nucleus ambiguus in the baroreflex arc. Therefore, targeting the nucleus ambiguus will lead to a focused direction to develop effective medical interventions for sleep apnea-induced cardiac neuropathy.

APPENDIX: FIGURES

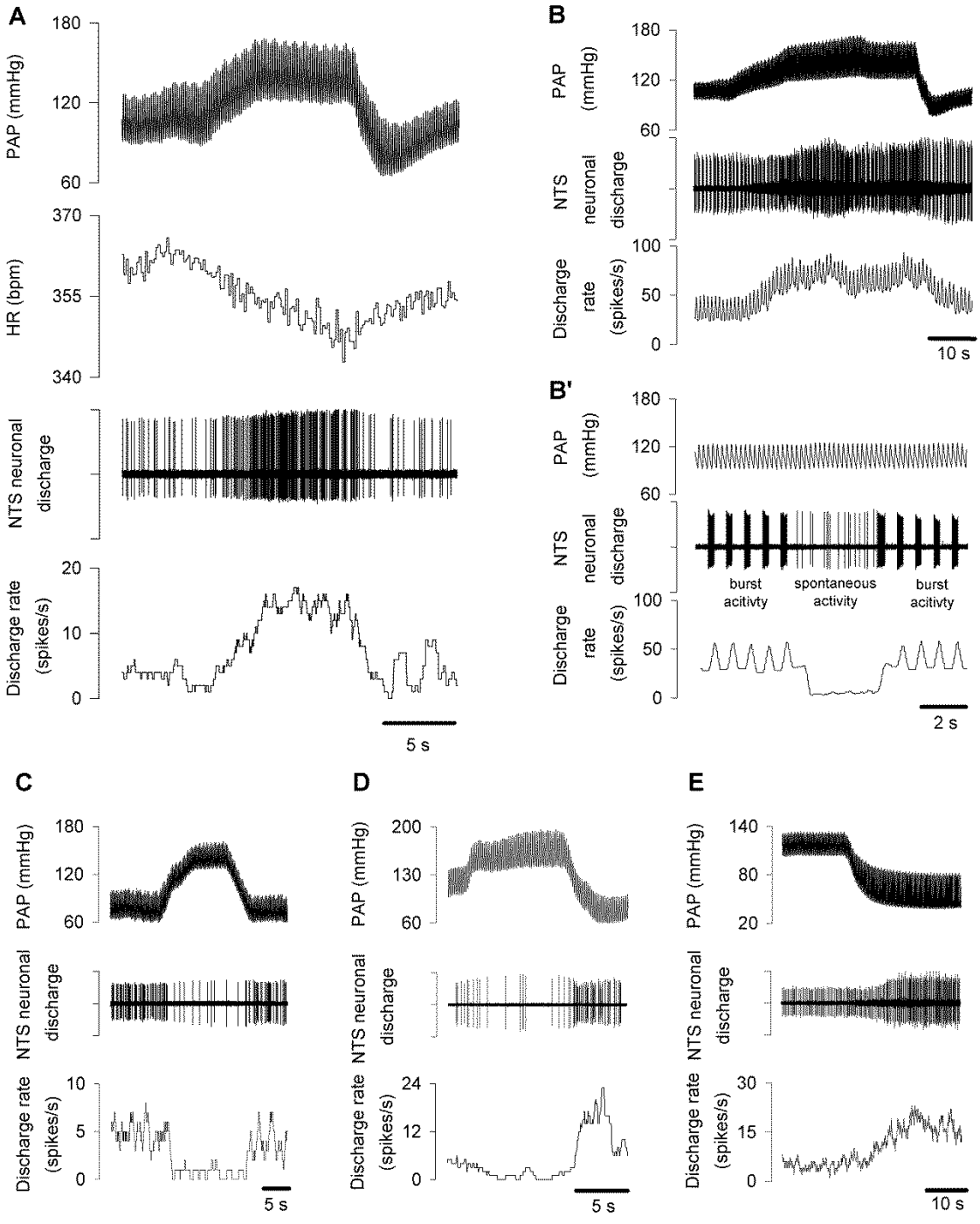
A
PAP (mmHg)
180
120
60
HR (bpm)
370
355
340
NTS neuronal discharge
Discharge rate (spikes/s)
20
10
0
5 s
B
PAP (mmHg)
180
120
60
NTS neuronal discharge
Discharge rate (spikes/s)
100
50
0
10 s
B'
PAP (mmHg)
180
120
60
NTS neuronal discharge
burst acitivty
spontaneous activity
burst acitivty
Discharge rate (spikes/s)
100
50
0
2 s
C
PAP (mmHg)
180
120
60
NTS neuronal discharge
Discharge rate (spikes/s)
10
5
0
5 s
D
PAP (mmHg)
200
130
60
NTS neuronal discharge
Discharge rate (spikes/s)
24
12
0
5 s
E
PAP (mmHg)
140
80
20
NTS neuronal discharge
Discharge rate (spikes/s)
30
15
0
10 s

Figure 1. NTS barosensitive neuronal activity in response to arterial pressure changes.

A) A representative excitatory neuron increased discharge rate in response to AP elevation. HR decreases in response to AP elevation. B) A pulmonary-related neuron. A representative excitatory neuron increased discharge rate during AP elevation. B') The same neurons as in panel B. The basal burst discharge of this neuron had a firing pattern which was synchronized with the rhythmic ventilation. When the ventilator was turned off for 3 s, this neuron lost the burst activity and instead the spontaneous activity appeared. The burst activity reappeared as the ventilator was turned back on. C) A representative NTS neuron decreased discharge rate during AP elevation. D) A representative NTS neuron had a bi-phasic response: first a decrease in discharge rate during AP elevation, then an increase in discharge rate during the descending phase of AP. E) A representative neuron was i.v. injected with sodium-nitroprusside (SNP) to decrease AP. SNP induced an excitatory response. HR: heart rate, PAP: pulse arterial pressure.

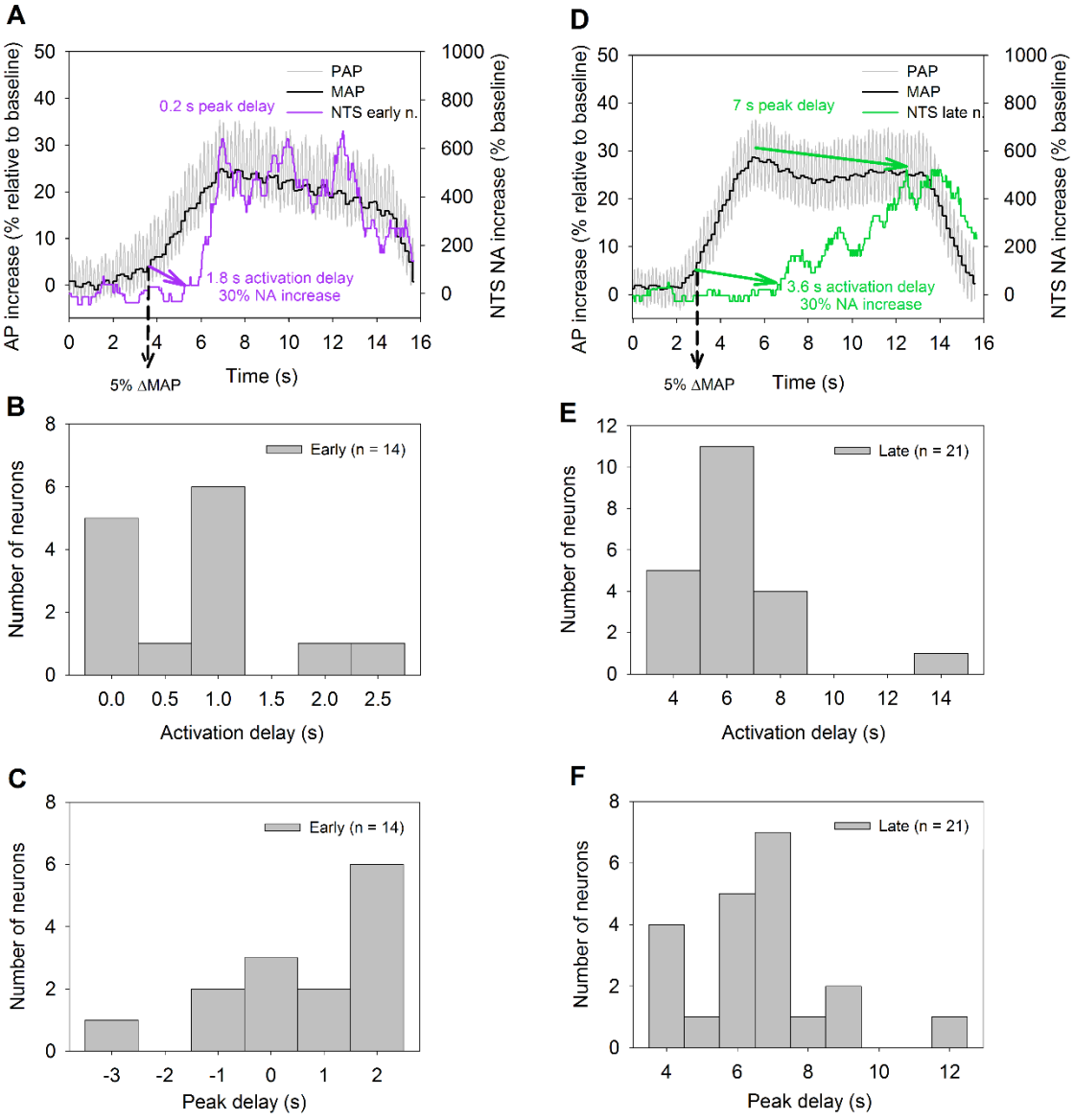
A
AP increase (% relative to baseline)
NTS NA increase (% baseline)
PAP
MAP
NTS early n.
0.2 s peak delay
1.8 s activation delay
30% NA increase
5% ΔMAP
Time (s)
D
PAP
MAP
NTS late n.
7 s peak delay
3.6 s activation delay
30% NA increase
5% ΔMAP
Time (s)
B
Number of neurons
Early (n = 14)
Activation delay (s)
E
Late (n = 21)
Activation delay (s)
C
Early (n = 14)
Peak delay (s)
F
Late (n = 21)
Peak delay (s)

Figure 2. Activation and peak delays of NTS early and late neuronal activity (NA).

AP increase (%) relative to baseline and NA increase (%) relative to the basal activity during AP elevation are superimposed on each other. 5% of MAP increase (ΔMAP) was defined as the MAP threshold. 30% of NA increase was defined as the NA activation threshold. The time period from 5% of MAP increase to 30% of NA increase was defined as NA activation delay. The period from the ΔMAP peak to NA peak increase was defined as the peak delay. A) A representative early neuronal activity (NA). The NA activation delay for this neuron was 1.8 s and the peak delay was 0.2 s. B) The distribution of the NA activation delay of the early neurons. C) The distribution of the peak delay of the early neurons. D) A representative NTS late NA. The NA activation delay for this neuron was 3.6 s and the peak delay was 7.0 s. E) The distribution of the NA activation delay of the late neurons. F) The distribution of the peak delay of the late neurons. The negative NA delay indicates the NA peak was before the ΔMAP peak.

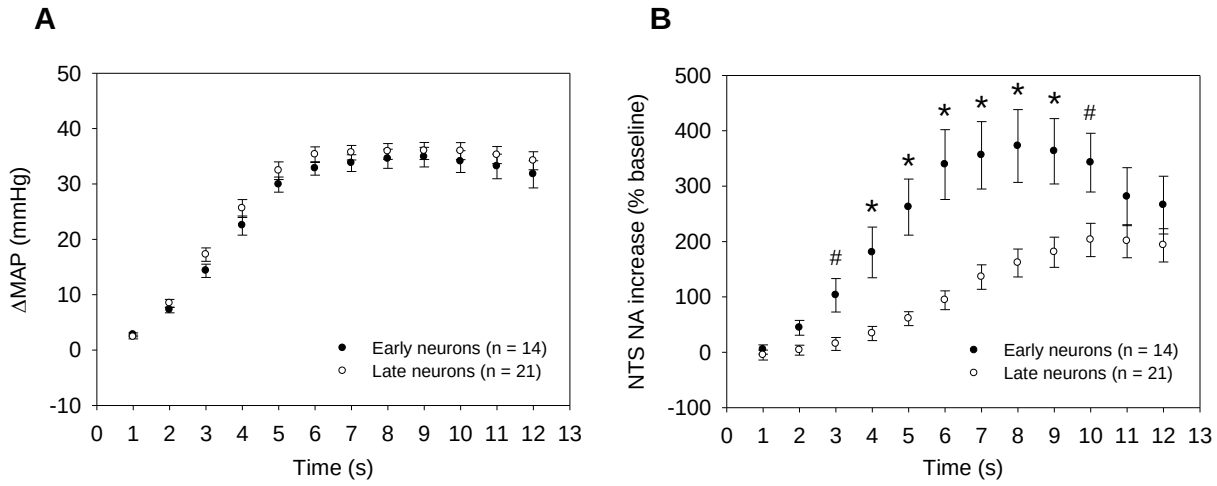

Figure 3. The time-course of NTS barosensitive neuronal activity (NA) increase in response to ΔMAP.

A) During 12 s descending aorta occlusion, early and late neurons had similar ΔMAP ($p>0.05$). B) During 12 s descending aorta occlusion, NA increase (%, relative to baseline) in early neurons had a significantly larger response in response to MAP increase than late neurons. (*$P<0.01$, $^{\#}P<0.05$)

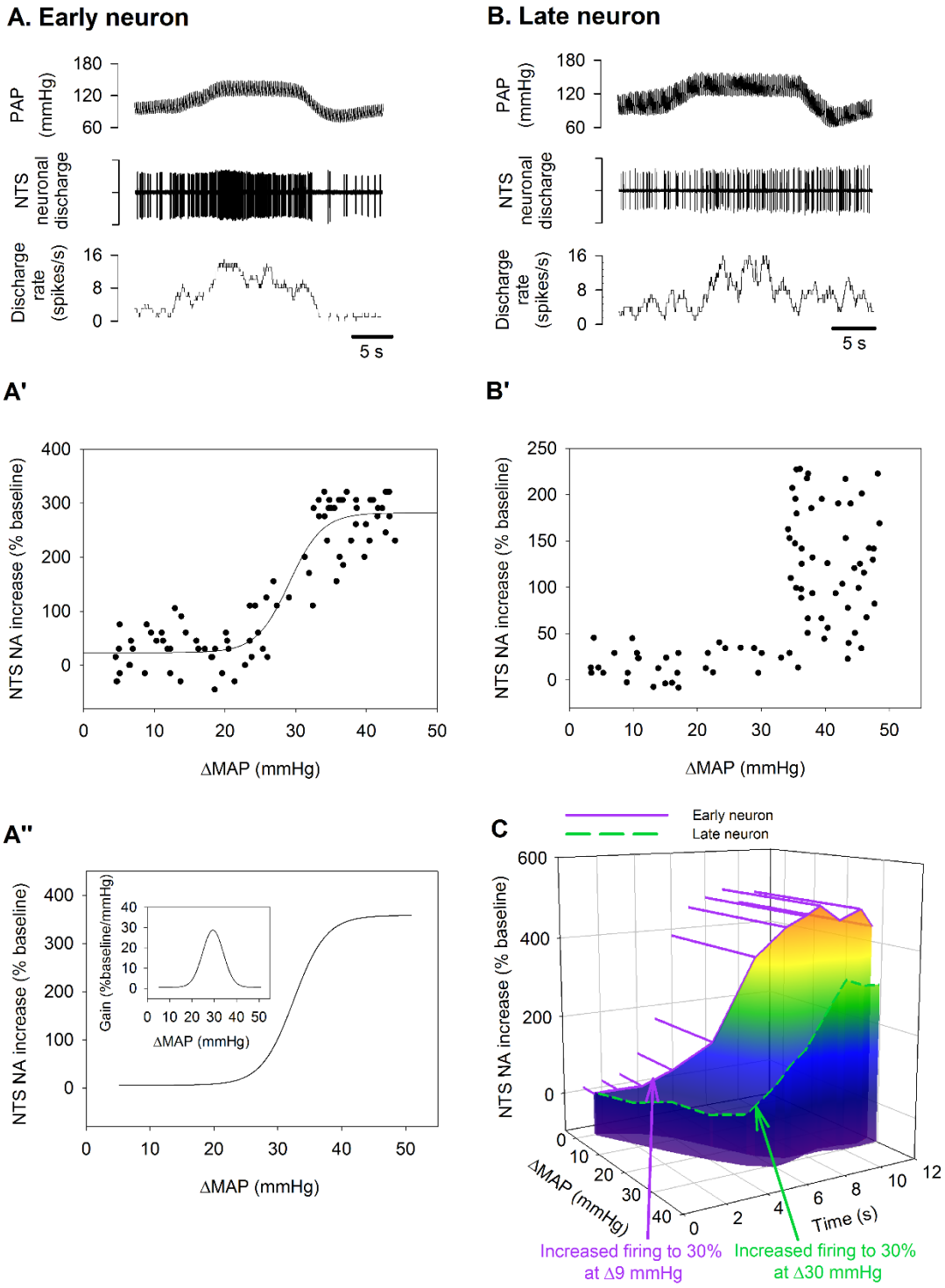
A. Early neuron
B. Late neuron
PAP (mmHg)
NTS neuronal discharge
Discharge rate (spikes/s)
5 s
A'
B'
NTS NA increase (% baseline)
ΔMAP (mmHg)
A''
Gain (%baseline/mmHg)
C
Early neuron
Late neuron
Time (s)
Increased firing to 30% at Δ9 mmHg
Increased firing to 30% at Δ30 mmHg

Figure 4. NTS neurons activity and ΔMAP relationship.

A) Original recordings of a representative early NA during MAP increase. A') The early NA-ΔMAP relationship curve was fitted using the the logistic sigmodal function. A'') The composite early NA - ΔMAP relationship curve was reconstructed using the averaged parameters of the logistic sigmodal function curves of 14 neurons as shown in Table 1. B) Original recordings of a representative late NA during MAP increase. B') This late neuron activity in reponse to MAP increase could not be fitted with the logistic sigmodal function curve because it did not increase firing rate until ΔMAP reached the peak (about 40 mmHg). C) A 3-D plot shows the different charateristic firing patterns of these two representative early and late neruons.

Table 1. Parameters defining the early neuronal activity (% baseline)-ΔMAP logistic function curve

R^2	A (range; mmHg)	B (slope coficient)	X_{50} (mmHg)	Y_{min} (%)	$Gain_{max}$ (%/mmHg)	X_{th} (mmHg)	X_{sat} (mmHg)
0.90±0.01	352.5±55.4	0.39±0.05	32.4±3.5	5.7±5.8	29.3±3.7	28.2±3.7	36.6±3.4

Values are means ± SE. n=14. R: correlation coefficient; A, maximum − minimum (range); X_{50}: slope coefficient; X_{50}, MAP at 50% of neuronal activity range; Y_{min}, mininal neruonal activity; Gmax, maximum early neruonal activity gain (slope); X_{th}, pressure threshold, $X_{50} - (1.317/ B)$; X_{sat}, pressure saturation, $X_{50} + (1.317/ B)$.

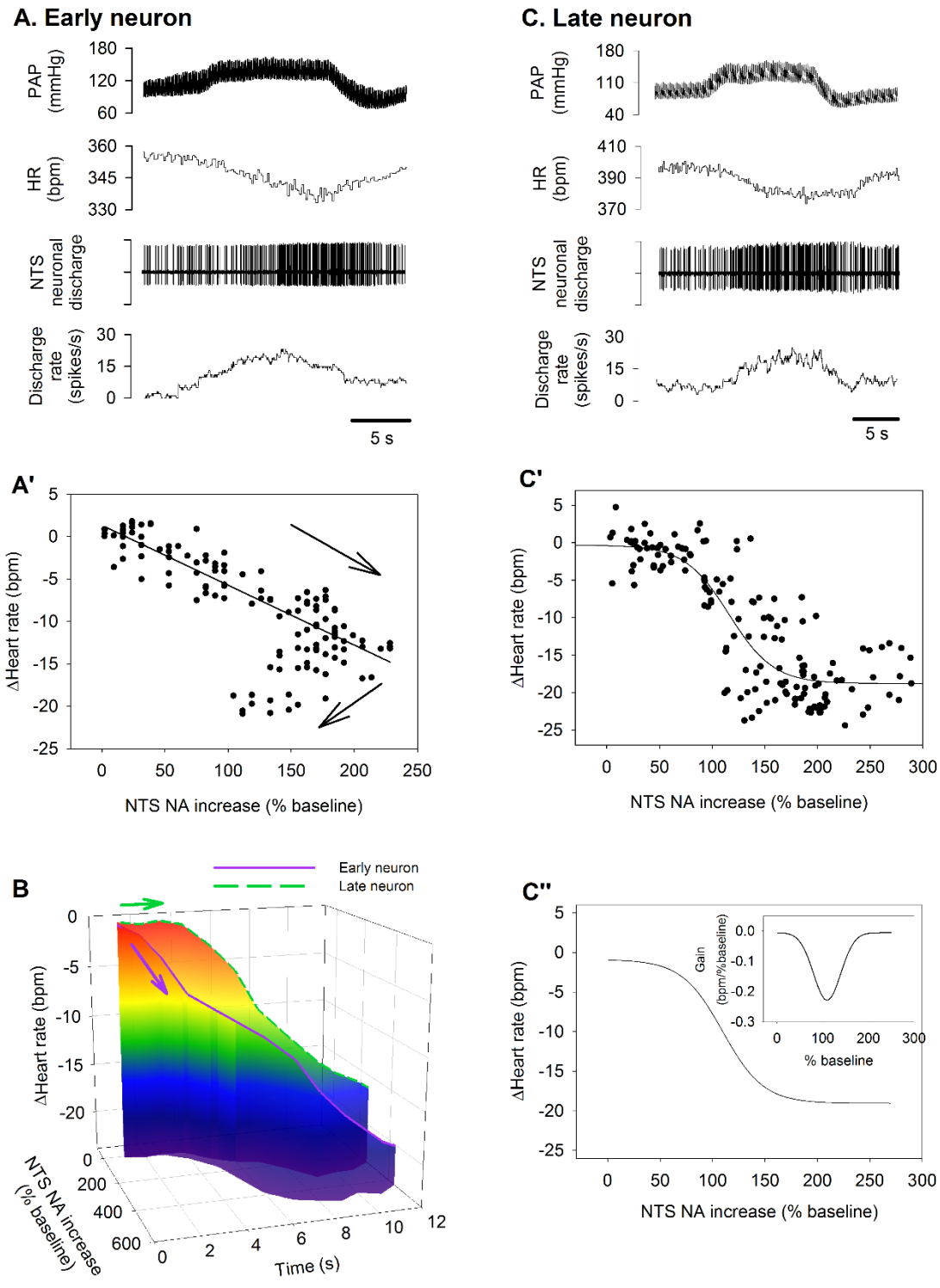
A. Early neuron
PAP (mmHg)
180
120
60
HR (bpm)
360
345
330
NTS neuronal discharge
Discharge rate (spikes/s)
30
15
0
5 s
C. Late neuron
PAP (mmHg)
180
110
40
HR (bpm)
410
390
370
NTS neuronal discharge
Discharge rate (spikes/s)
30
15
0
5 s
A'
ΔHeart rate (bpm)
5
0
-5
-10
-15
-20
-25
0
50
100
150
200
250
NTS NA increase (% baseline)
C'
ΔHeart rate (bpm)
5
0
-5
-10
-15
-20
-25
0
50
100
150
200
250
300
NTS NA increase (% baseline)
B
Early neuron
Late neuron
ΔHeart rate (bpm)
0
-5
-10
-15
-20
NTS NA increase (% baseline)
0
200
400
600
Time (s)
0
2
4
6
8
10
12
C''
ΔHeart rate (bpm)
5
0
-5
-10
-15
-20
-25
Gain (bpm/%baseline)
0.0
-0.1
-0.2
-0.3
0
100
200
300
% baseline
0
50
100
150
200
250
300
NTS NA increase (% baseline)

Figure 5. Heart rate and NTS neurons activity relationship.

A) Original recordings of a representative early neuron activity and the HR reduction during MAP increase. A') The initial HR reduction was linearly correlated with the increase of this early NA till the peak firing (about 200% relative to the baseline). After the peak firing, this neuron activity declined while the HR was still decreasing. B) A 3-D plot shows the difference of the HR reduction- NA between two representative early and late neurons as shown in Fig.4. Whereas the early neuron contributed to the initial HR reduction, the late neuron did not contribute to HR reduction until a late time. C) Original recordings of a representative late neuron activity and the HR reduction during MAP increase. C') The HR and this late NA relationship curve was fitted using the logistic sigmodal function. C'') The composite HR-late NA relationship curve was reconstructed using the averaged parameters of the logistic sigmodal function curves of 21 neurons as shown in Table 2.

Table 2. Parameters defining heart rate reduction (ΔHR)-late neuronal activity (NA, % baseline)-logistic function curve.

R^2	A (range; %)	B (slope coefficient)	X_{50} (%)	Y_{max} (bpm)	$Gain_{max}$ (bpm/%)	X_{th} (%)	X_{sat} (%)
0.75 ±0.01	18.9 ±1.2	-0.04 ±0.006	111.8 ±18.4	-21.2 ±1.3	-0.23 ±0.04	67.3 ±12.9	156.3 ±24.3

Values are means ± SE. n=21. R: correlation coefficient; A, minimum- maximum (range); X_{50}: slope coefficient; X_{50}, NA at 50% of HR reduction range; Y_{max}, maximum neruonal activity; G_{max}, maximum HR reduction gain (slope); X_{th}, NA threshold, X_{50} + (1.317/ B); X_{sat}, NA saturation, X_{50} - (1.317/ B).

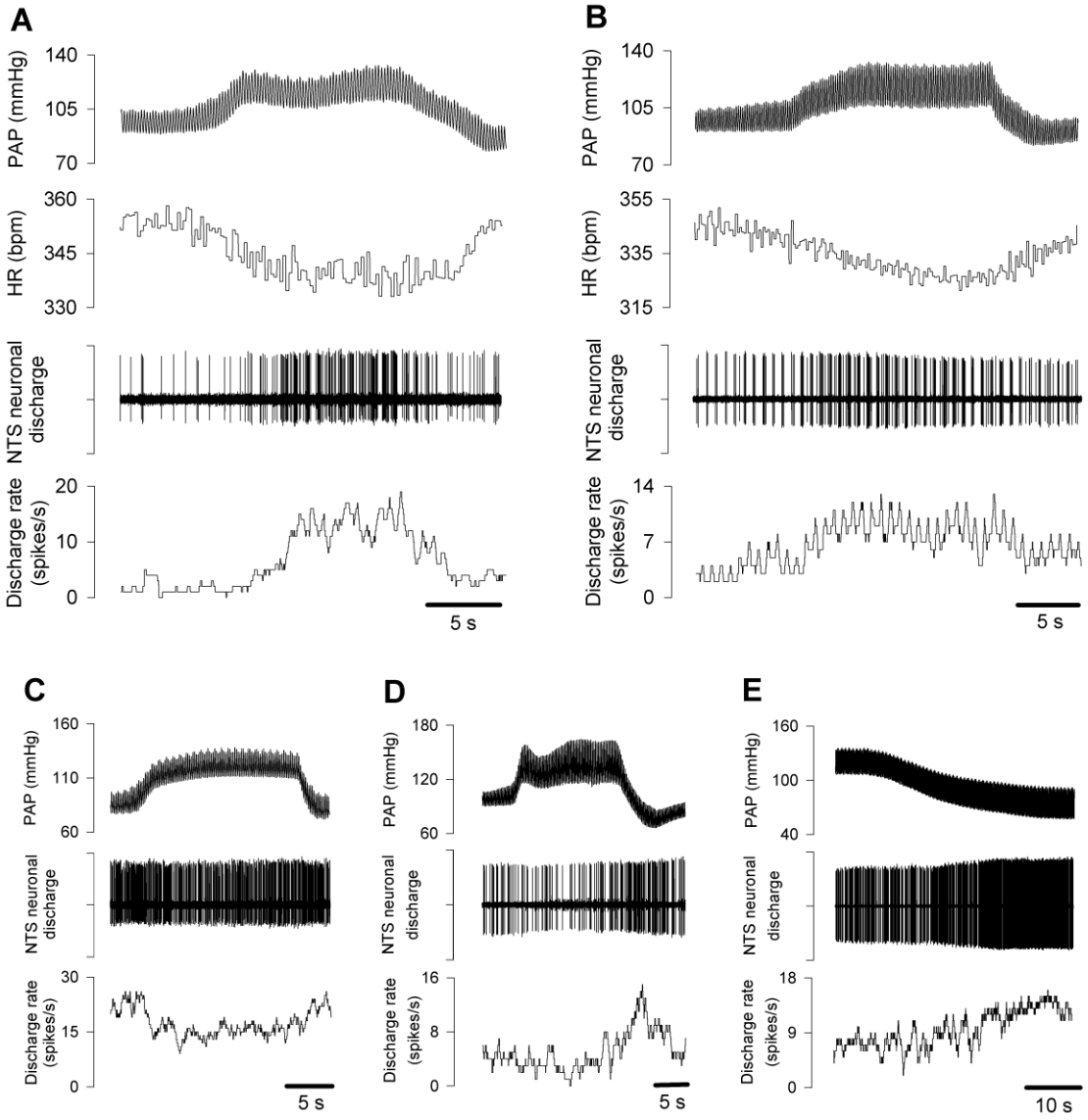
A
PAP (mmHg)
140
105
70
HR (bpm)
360
345
330
NTS neuronal discharge
Discharge rate (spikes/s)
20
10
0
5 s
B
PAP (mmHg)
140
105
70
HR (bpm)
355
335
315
NTS neuronal discharge
Discharge rate (spikes/s)
14
7
0
5 s
C
PAP (mmHg)
160
110
60
NTS neuronal discharge
Discharge rate (spikes/s)
30
15
0
5 s
D
PAP (mmHg)
180
120
60
NTS neuronal discharge
Discharge rate (spikes/s)
16
8
0
5 s
E
PAP (mmHg)
160
100
40
NTS neuronal discharge
Discharge rate (spikes/s)
18
9
0
10 s

Figure 6. NTS barosensitive neuronal activity in response to arterial pressure changes in Ketamine-anesthetized rats.

A) A representative excitatory neuron increased discharge rate in response to AP elevation. HR decreases in response to AP elevation. B) A pulmonary-related neuron that increased discharge rate during AP elevation. The basal burst discharge of this neuron had a firing pattern which was synchronized with the rhythmic ventilation. C) A representative NTS neuron decreased discharge rate during AP elevation. D) A representative NTS neuron increased discharge during AP decrease. E) A representative neuron was i.v. injected with sodium-nitroprusside (SNP) to decrease AP: SNP induced an excitatory response. HR: heart rate, PAP: pulse arterial pressure.

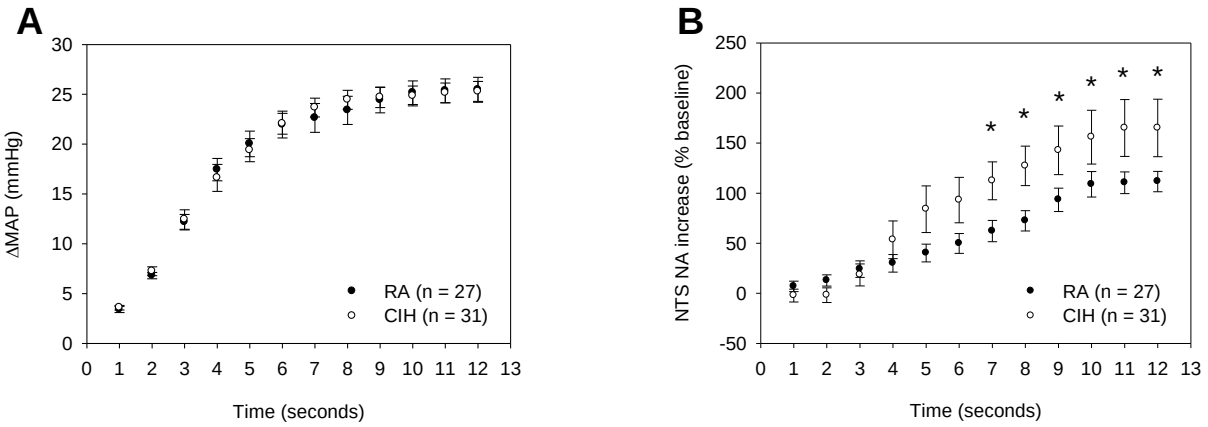

Figure 7. The time-course of RA and CIH NTS barosensitive neuronal activity (NA) in response to ΔMAP.

A) During 12 s descending aorta occlusion, 27 room air (RA) and 31 chronic intermittent hypoxia (CIH) neurons had similar ΔMAP ($p>0.05$). B) During 7-12 s of descending aorta occlusion ΔMAP in 2A, CIH NA increase (% relative to baseline, n = 31) was significantly larger than RA NA increase (n = 27, *$P<0.05$)

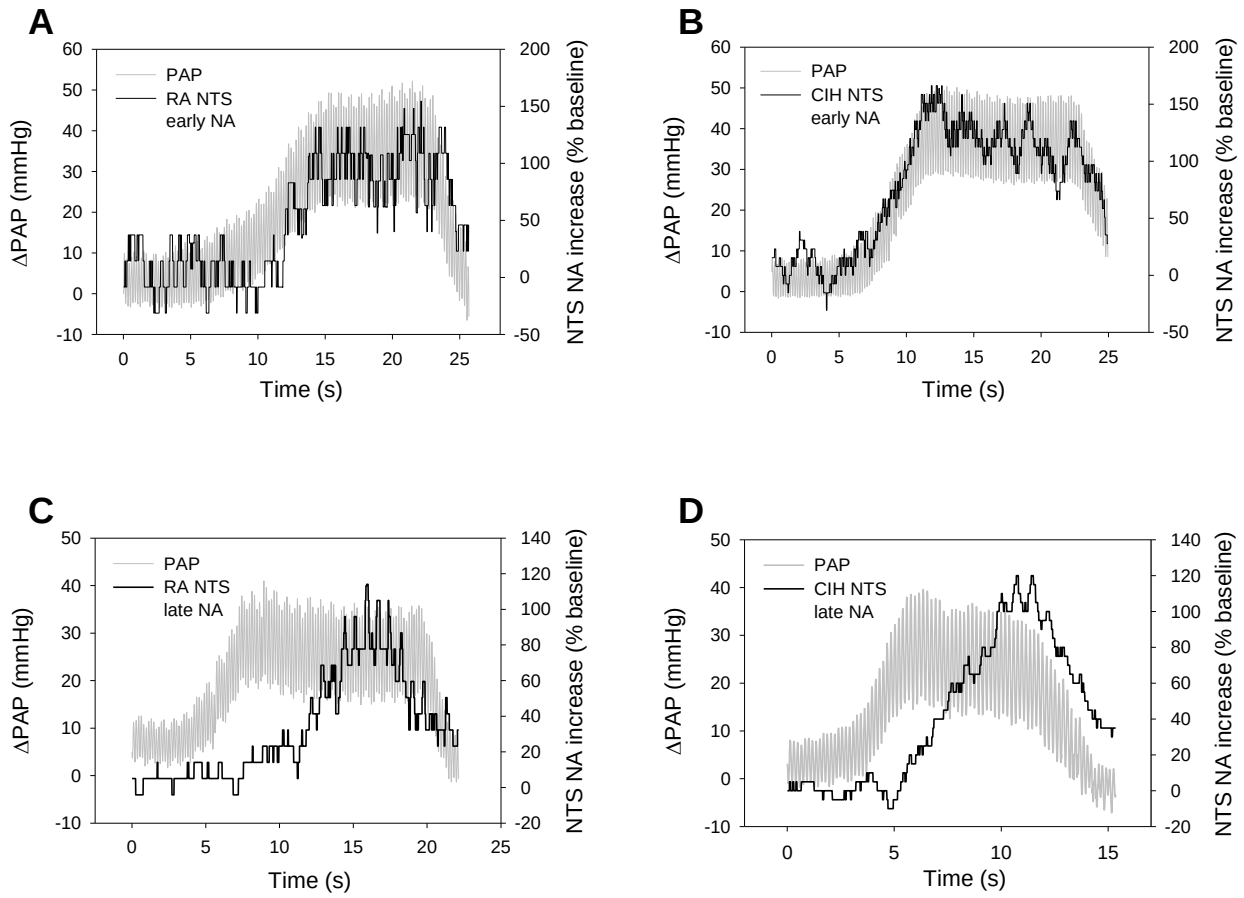

Figure 8. Activation delay of NTS early and late neuronal activity (NA) in RA and CIH neurons.

PAP increase (mmHg, max response-baseline) and NA increase (%) relative to the basal activity during AP elevation are superimposed on each other. 30% of NA increase was defined as the NA activation threshold. A representative original recordings of RA (A) and CIH (B) neurons which increased NA simultaneously with MAP increase. A representative original recordings of RA (C) and CIH (D) late neurons which increased NA only at or after AP maximum.

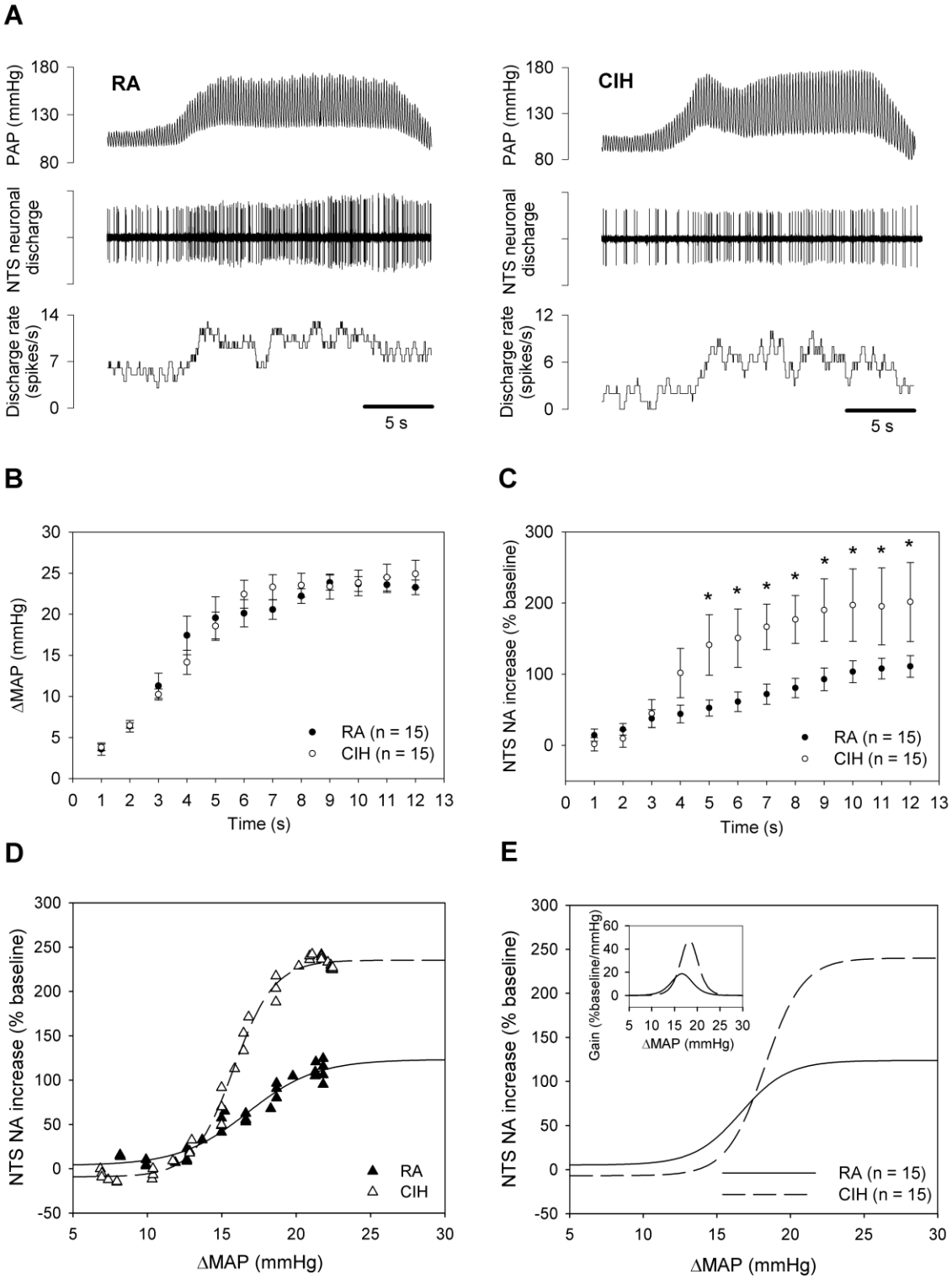
A
RA
CIH
PAP (mmHg)
180
130
80
NTS neuronal discharge
Discharge rate (spikes/s)
14
7
0
12
6
5 s
B
ΔMAP (mmHg)
30
25
20
15
10
5
0
0 1 2 3 4 5 6 7 8 9 10 11 12 13
Time (s)
RA (n = 15)
CIH (n = 15)
C
NTS NA increase (% baseline)
300
200
100
0
*
Time (s)
D
NTS NA increase (% baseline)
300
250
200
150
100
50
0
-50
5 10 15 20 25 30
ΔMAP (mmHg)
RA
CIH
E
Gain (%baseline/mmHg)
60
40
20
0
5 10 15 20 25 30
ΔMAP (mmHg)

Figure 9. Early NTS neurons' activity and ΔMAP relationship in RA and CIH neurons.

A) Original recordings of a representative early RA and CIH NAs during MAP increase. B) The time-course of ΔMAP during 12 s descending aorta occlusion. C) The time-course of 15 RA and 15 CIH NA increase (% relative to baseline) in response to ΔMAP in (B). During 5-12 s of ΔMAP, CIH NA increase (n = 15) was significantly larger than RA NA increase (n = 15, *P <0.05). D) The early NA-ΔMAP relationship curve was fitted using the the logistic sigmodal function. E) The composite early NA-ΔMAP relationship curves were reconstructed using the averaged parameters of the logistic sigmodal function curves of 15 RA and 15 CIH neurons as shown in Table 1.

Table 3. Parameters defining the early neuronal activity (% baseline)–ΔMAP logistic function curves for RA and CIH neurons.

	A (range; mmHg)	B (slope coefficient)	X_{50} (mmHg)	Y_{min} (%)	$Gain_{max}$ (%/mmHg)	X_{th} (mmHg)	X_{sat} (mmHg)	R^2
RA n = 15	118.4 ±21.6	0.63 ±0.08	16.6 ±1.8	5.3 ±7.9	19.1 ±4.2	14.0 ±1.6	19.2 ±1.9	0.90± 0.01
CIH n =15	246.8 ±55.5	0.77 ±0.15	18.2 ±1.8	-6.8 ±17.6	47.7 ±12.6	15.2 ±2.3	21.2 ±1.4	0.88± 0.01
	P<0.05	N.S.	N.S.	N.S.	P<0.05	N.S.	N.S.	

Values are means ± SE. R^2, correlation coefficient; A, maximum − minimum (range); B, slope coefficient; X_{50}, MAP at 50% of neruonal activity range; Y_{min}, mininal neruonal activity; $Gain_{max}$, maximum early neruonal activity gain (slope); X_{th}, $X_{50} - (1.317/ B)$; X_{sat}, $X_{50} + (1.317/ B)$.

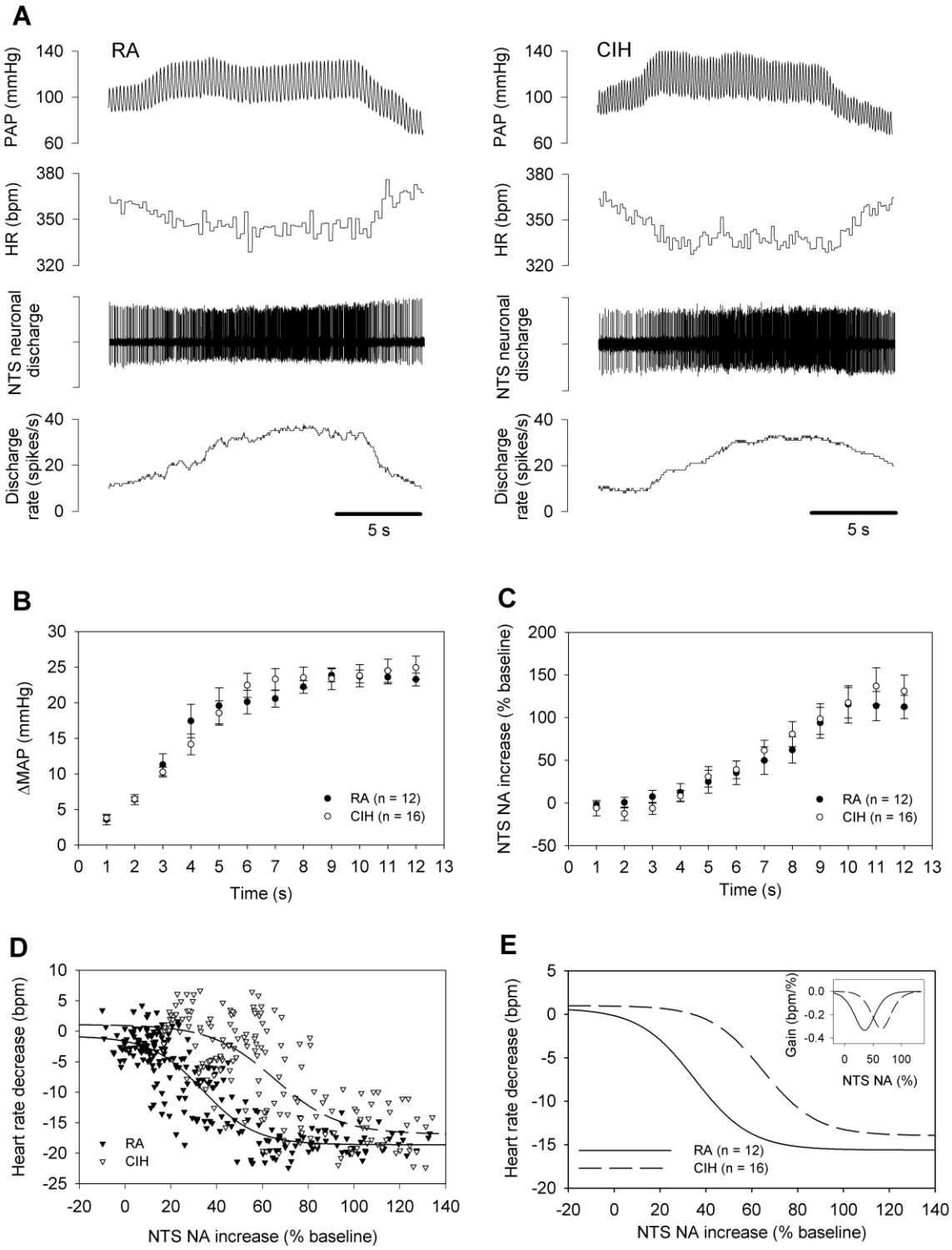
A
RA
CIH
PAP (mmHg)
HR (bpm)
NTS neuronal discharge
Discharge rate (spikes/s)
5 s
B
ΔMAP (mmHg)
Time (s)
RA (n = 12)
CIH (n = 16)
C
NTS NA increase (% baseline)
Time (s)
RA (n = 12)
CIH (n = 16)
D
Heart rate decrease (bpm)
NTS NA increase (% baseline)
RA
CIH
E
Heart rate decrease (bpm)
NTS NA increase (% baseline)
Gain (bpm/%)
NTS NA (%)
RA (n = 12)
CIH (n = 16)

Figure 10. Late NTS neurons' activity–ΔMAP and late NTS neurons' activity–ΔHR relationships for RA and CIH neurons.

A) Original recordings of a representative late RA and CIH NAs and the HR reduction during MAP increase. B) The time-course of ΔMAP during 12 s descending aorta occlusion. C) The time-course of 12 RA and 16 CIH NA increase (% relative to baseline) in response to ΔMAP in (B). During 12 s of ΔMAP there was no difference between CIH (n = 16) and RA (n = 12) NA increase (P>0.05). D) The HR-late NA relationship curve from RA and CIH neurons was fitted using the logistic sigmodal function. E) The composite HR-late NA relationship curves were reconstructed using the averaged parameters of the logistic sigmodal function curves of 12 RA and 16 CIH neurons as shown in Table 2.

Table 4. Parameters defining heart rate reduction (ΔHR)–late neuronal activity (NA, % baseline)–logistic function curves for RA and CIH neurons.

	A (range; %)	B (slope coefficient)	X_{50} (%)	Y_{max} (bpm)	$Gain_{max}$ (bpm/%)	X_{th} (%)	X_{sat} (%)	R^2
RA n = 12	16.3 ±1.6	-0.082 ±0.027	35.1 ±6.2	17.0 ±1.0	-0.33 ±0.061	61.9 ±8.0	8.3 ±9.5	0.74 ±0.02
CIH n =16	14.9 ±1.5	-0.085 ±0.021	64.9 ±11.9	15.9 ±1.0	-0.30 ±0.060	87.6 ±12.6	42.2 ±12.6	0.76 ±0.03
	N.S.	N.S.	P<0.05	N.S.	N.S.	N.S.	P<0.05	

Values are means ± SE. R^2, correlation coefficient; A, minimum-maximum (range); B, slope coefficient; X_{50}, NA at 50% of HR reduction range; Y_{max}, maximum neruonal activity; $Gain_{max}$, maximum HR reduction gain (slope); X_{th}, X_{50} + (1.317/ B); X_{sat}, X_{50} - (1.317/ B).

LIST OF REFERENCES

Ai J, Wurster RD, Harden SW, Cheng ZJ (2009) Vagal afferent innervation and remodeling in the aortic arch of young-adult fischer 344 rats following chronic intermittent hypoxia. Neuroscience 164:658-666.

Almado CEL, Accorsi-Mendonca D, Machado BH, Leao RMX (2008) Chronic intermittent hypoxia (CIH) enhances spontaneous synaptic transmission in the nucleus tractus solitarii (NTS) neurons of juvenile rats. Faseb Journal 22:1.

Almado CE, Machado BH, Leao RM (2012) Chronic intermittent hypoxia depresses afferent neurotransmission in NTS neurons by a reduction in the number of active synapses. J Neurosci 32:16736-16746.

Andresen MC, Kunze DL (1994) Nucleus Tractus Solitarius – Gateways to Neural Circulatory Control. Annual Review of Physiology 56:93-116.

Andresen MC, Doyle MW, Bailey TW, Jin YH (2004) Differentiation of autonomic reflex control begins with cellular mechanisms at the first synapse within the nucleus tractus solitarius. Brazilian Journal of Medical and Biological Research 37:549-558.

Andresen MC, Peters JH (2008) Comparison of baroreceptive to other afferent synaptic transmission to the medial solitary tract nucleus. American Journal of Physiology-Heart and Circulatory Physiology 295:H2032-H2042.

Bonsignore MR, Parati G, Insalaco G, Castiglioni P, Marrone O, Romano S, Salvaggio A, Mancia G, Bonsignore G, Di Rienzo M (2006) Baroreflex control of heart rate during sleep in severe obstructive sleep apnoea: effects of acute CPAP. European Respiratory Journal 27:128-135.

Bradley TD, Floras JS (2009) Obstructive sleep apnoea and its cardiovascular consequences. Lancet 373:82-93.

Brown AM (1980) Receptors Under Pressure - Update on Baroreceptors. Circulation Research 46:1-10.

Chen M, Yang M, Han W, An S, Liu Y, Liu Z, Ren W (2014) Individual aortic baroreceptors are sensitive to different ranges of blood pressures. Science China-Life Sciences 57:502-509.

Costa-Silva JH, Zoccal DB, Machado BH (2012) Chronic intermittent hypoxia alters glutamatergic control of sympathetic and respiratory activities in the commissural NTS of rats. Am J Physiol Regul Integr Comp Physiol 302:R785-793.

de Paula PM, Tolstykh G, Mifflin S (2007) Chronic intermittent hypoxia alters NMDA and AMPA-evoked currents in NTS neurons receiving carotid body chemoreceptor inputs. Am J Physiol Regul Integr Comp Physiol 292:R2259-2265.

Deuchars J, Li YW, Kasparov S, Paton JFR (2000) Morphological and electrophysiological

properties of neurones in the dorsal vagal complex of the rat activated by arterial baroreceptors. Journal of Comparative Neurology 417:233-249.

Doyle MW, Andresen MC (2001) Reliability of monosynaptic sensory transmission in brain stem neurons in vitro. Journal of Neurophysiology 85:2213-2223.

Gozal D, Daniel JM, Dohanich GP (2001) Behavioral and anatomical correlates of chronic episodic hypoxia during sleep in the rat. Journal of Neuroscience 21:2442-2450.

Gu H, Lin M, Liu J, Gozal D, Scrogin KE, Wurster R, Chapleau MW, Ma X, Cheng ZJ (2007) Selective impairment of central mediation of baroreflex in anesthetized young adult Fischer 344 rats after chronic intermittent hypoxia. American journal of physiology Heart and circulatory physiology 293:H2809-2818.

Gu H, Epstein PN, Li L, Wurster RD, Cheng ZJ (2008) Functional Changes in Baroreceptor Afferent, Central, and Efferent Components of the Baroreflex Circuitry in Type 1 Diabetic Mice (OVE26). Faseb Journal 22.

Kline DD, Ramirez-Navarro A, Kunze DL (2007) Adaptive depression in synaptic transmission in the nucleus of the solitary tract after in vivo chronic intermittent hypoxia: Evidence for homeostatic plasticity. Journal of Neuroscience 27:4663-4673.

Kline DD (2008) Plasticity in glutamatergic NTS neurotransmission. Respiratory Physiology & Neurobiology 164:105-111.

Kline DD (2010) Chronic intermittent hypoxia affects integration of sensory input by neurons in the nucleus tractus solitarii. Respir Physiol Neurobiol 174:29-36.

Lai CJ, Yang CCH, Hsu YY, Lin YN, Kuo TBJ (2006) Enhanced sympathetic outflow and decreased baroreflex sensitivity are associated with intermittent hypoxia-induced systemic hypertension in conscious rats. Journal of applied physiology 100:1974-1982.

Lin M, Liu R, Gozal D, Wead WB, Chapleau MW, Wurster R, Cheng ZJ (2007) Chronic intermittent hypoxia impairs baroreflex control of heart rate but enhances heart rate responses to vagal efferent stimulation in anesthetized mice. American journal of physiology Heart and circulatory physiology 293:H997-1006.

Lin M, Ai J, Li L, Huang C, Chapleau MW, Liu R, Gozal D, Wead WB, Wurster RD, Cheng Z (2008) Structural remodeling of nucleus ambiguus projections to cardiac ganglia following chronic intermittent hypoxia in C57BL/6J mice. J Comp Neurol 509:103-117.

Monahan KD, Lettenberger UA, Ray CA (2006) Effect of repetitive hypoxic apnoeas on baroreflex function in humans. Journal of Physiology-London 574:605-613.

Ott MM, Nuding SC, Segers LS, Lindsey BG, Morris KF (2011) Ventrolateral medullary functional connectivity and the respiratory and central chemoreceptor-evoked modulation of retrotrapezoid-parafacial neurons. Journal of Neurophysiology 105:2960-2975.

Parati G, Di Rienzo M, Bonsignore MR, Insalaco G, Marrone O, Castiglioni P, Bonsignore G,

Mancia G (1997) Autonomic cardiac regulation in obstructive sleep apnea syndrome: evidence from spontaneous baroreflex analysis during sleep. Journal of hypertension 15:1621-1626.

Paton JFR (1998) Pattern of cardiorespiratory afferent convergence to solitary tract neurons driven by pulmonary vagal C-fiber stimulation in the mouse. Journal of Neurophysiology 79:2365-2373.

Paton JFR, Li YW, Schwaber JS (2001) Response properties of baroreceptive NTS neurons. In: Neuro-Cardiovascular Regulation: from Molecules to Man, vol. 940 (Chapleau, M. W. and Abboud, F. M., eds), pp 157-168.

Potts JT (2002) Neural circuits controlling cardiorespiratory responses: Baroreceptor and somatic afferents in the nucleus tractus solitarius. Clinical and Experimental Pharmacology and Physiology 29:103-111.

Potts JT (2006) Inhibitory neurotransmission in the nucleus tractus solitarii: implications for baroreflex resetting during exercise. Experimental physiology 91:59-72.

Reeves SR, Guo SZ, Brittian KR, Row BW, Gozal D (2006) Anatomical changes in selected cardio-respiratory brainstem nuclei following early post-natal chronic intermittent hypoxia. Neuroscience Letters 402:233-237.

Rogers RF, Paton JF, Schwaber JS (1993) NTS neuronal responses to arterial pressure and

pressure changes in the rat. The American journal of physiology 265:R1355-1368.

Rogers RF, Rose WC, Schwaber JS (1996) Simultaneous encoding of carotid sinus pressure and dP/dt by NTS target neurons of myelinated baroreceptors. Journal of Neurophysiology 76:2644-2660.

Rogers RF, Rybak IA, Schwaber JS (2000) Computational modeling of the baroreflex arc: Nucleus tractus solitarius. Brain Research Bulletin 51:139-150.

Roux F, D'Ambrosio C, Mohsenin V (2000) Sleep-related breathing disorders and cardiovascular disease. American Journal of Medicine 108:396-402.

Seagard JL, Vanbrederode JFM, Dean C, Hopp FA, Gallenberg LA, Kampine JP (1990) Firing characteristics of single-fiber carotid-sinus baroreceptors. Circulation Research 66:1499-1509.

Seagard JL, Dean C, Hopp FA (1995) Discharge patterns of baroreceptor-modulated neurons in the Nucleus Tractus Solitarius. Neuroscience letters 191:13-18.

Seagard JL, Dean C, Hopp FA (2001) Properties of NTS neurons receiving input from barosensitive receptors. Neuro-Cardiovascular Regulation: from Molecules to Man 940:142-156.

Striedter G (2014) Regulating Vital Bodily Functions. In: Functional Neurobiology, 1st Edition:

Oxford University Press.

Wang WZ, Gao L, Pan YX, Zucker IH, Wang W (2006) Differential effects of cardiac sympathetic afferent stimulation on neurons in the nucleus tractus solitarius. Neurosci Lett 409:146-150.

Wang WZ, Gao L, Pan YX, Zucker IH, Wang W (2007) AT1 receptors in the nucleus tractus solitarii mediate the interaction between the baroreflex and the cardiac sympathetic afferent reflex in anesthetized rats. Am J Physiol Regul Integr Comp Physiol 292:R1137-1145.

Wang WZ, Gao L, Wang HJ, Zucker IH, Wang W (2008) Interaction between cardiac sympathetic afferent reflex and chemoreflex is mediated by the NTS AT1 receptors in heart failure. Am J Physiol Heart Circ Physiol 295:H1216-H1226.

Wu Q, Mifflin S (2014) Time course of changes in glutamatergic transmission within NTS during CIH exposure and the role of Delta FosB. Faseb Journal 28.

Yamamoto K, Eubank W, Franzke M, Mifflin S (2013) Resetting of the sympathetic baroreflex is associated with the onset of hypertension during chronic intermittent hypoxia. Auton Neurosci 173:22-27.

Yan B, Li L, Harden SW, Gozal D, Lin Y, Wead WB, Wurster RD, Cheng ZJ (2009) Chronic

intermittent hypoxia impairs heart rate responses to AMPA and NMDA and induces loss of glutamate receptor neurons in nucleus ambiguous of F344 rats. American journal of physiology Regulatory, integrative and comparative physiology 296:R299-308.

Yan B, Soukhova-O'Hare GK, Li L, Lin Y, Gozal D, Wead WB, Wurster RD, Cheng ZJ (2008) Attenuation of heart rate control and neural degeneration in nucleus ambiguus following chronic intermittent hypoxia in young adult Fischer 344 rats. Neuroscience 153:709-720.

Young T, Peppard P, Palta M, Hla KM, Finn L, Morgan B, Skatrud J (1997) Population-based study of sleep-disordered breathing as a risk factor for hypertension. Archives of Internal Medicine 157:1746-1752.

Zhang J, Mifflin SW (2000a) Responses of aortic depressor nerve-evoked neurones in rat nucleus of the solitary tract to changes in blood pressure. Journal of Physiology-London 529:431-443.

Zhang J, Mifflin SW (2000b) Subthreshold aortic nerve inputs to neurons in nucleus of the solitary tract. American Journal of Physiology-Regulatory Integrative and Comparative Physiology 278:R1595-R1604.

Zhang W, Carreno FR, Cunningham JT, Mifflin SW (2008) Chronic sustained and intermittent hypoxia reduce function of ATP-sensitive potassium channels in nucleus of the solitary tract. Am J Physiol Regul Integr Comp Physiol 295:R1555-1562.

Zhang XG, Cui JJ, Tan ZJ, Jiang CH, Fogel R (2003) The central nucleus of the amygdala modulates gut-related neurons in the dorsal vagal complex in rats. Journal of Physiology-London 553:1005-1018.

Zhang XG, Fogel R (2003) Involvement of glutamate in gastrointestinal vago-vagal reflexes initiated by gastrointestinal distention in the rat. Autonomic Neuroscience-Basic & Clinical 103:19-37.

Zoccal DB, Bonagamba LG, Paton JF, Machado BH (2009) Sympathetic-mediated hypertension of awake juvenile rats submitted to chronic intermittent hypoxia is not linked to baroreflex dysfunction. Exp Physiol 94:972-983.